A

Dissertation Phase -II Report

On

Design and Development of Geothermal Air Conditioning test rig

By

MR.PIYUSH PRATAP PATIL

(121M1J001)

Submitted in partial fulfillment for the degree of

M.Tech Mechanical (Heat Power Engineering)

Under the guidance of

PROF. DR. ABHAY LINGAYAT
PROF. DR. JAYA GOYAL

Mechanical Engineering Department

Pimpri Chinchwad College of Engineering, Pune
(An Autonomous Institute approved by UGC and Affiliated to SPPU)

June, 2023

Declaration

I declare that this written submission represents my ideas in my own words and where others' ideas or words have been included, I have adequately cited and referenced the original sources. I also declare that I have adhered to all principles of academic honesty and integrity and have not misrepresented or fabricated or falsified any idea/data/fact/source in my submission. I understand that any violation of the above will be cause for disciplinary action by the Institute and can also evoke penal action from the sources which have thus not been properly cited or from whom proper permission has not been taken when needed.

____

DR. ABHAY LINGAYAT

____

MR. PIYUSH PRATAP PATIL

(121M1J001

Date: __________

C E R T I F I C A T E

This is to certify that Mr. Piyush Pratap Patil, has successfully completed the Dissertation phase-II titled “Design and Development of Geothermal Air Conditioning test rig” under my supervision, in the partial fulfillment of Master of Technology- Mechanical Engineering (Heat Power Engineering) of Savitribai Phule Pune University.

Date:

Place: PCCOE, Nigdi.

----------------------------------	---------------------------------
Dr. Abhay Lingayat	Dr. P.A. Deshmukh Head Mechanical Engineering Department
----------------------------------	---------------------------------
External Examiner	Director

Acknowledgement

I wish to express my deep sense of gratitude and honor towards my respected guide Dr. Abhay Lingayat and Dr. Jaya Goyal for their inspiring guidance and constant encouragement. Their committed devotion, dedication and encouragement with full faith on me were like a lamp in my path which keeps me constant throughout project work.

Special thanks to Dr. Abhay Lingayat and Dr. Jaya Goyal for their guidance and support at various stages during the course of my project completion. I would like to thank ISHRAE and Pimpri Chinchwad College of engineering for providing financial assistance for the project.

I also express my honor and gratitude to Professor and Head of Mechanical Department Dr. P.A. Deshmukh for consistent encouragement for completing my project work successfully. I am thankful to all Teaching and Non-Teaching staff member of the institute who had directly or indirectly made me enthusiastic for the project work.

As I conclude, I would like to state that just as a positive attitude pays off my hard efforts to bring this project to successful end, would also pay off. I hope that this project would be one of the most significant steeping stones for my career and would fulfill my aspiration in every aspect.

PROJECTEE

MR. PIYUSH PATIL

Abstract

The Geothermal air conditioner is a passive technique which can help in reducing the heating/cooling load of a space which is to be conditioned. At a certain depth temperature of the ground remains constant, this temperature is higher in case of winter season and lower in case of summer season. The practical implementation of such system is bit costly and the performance of the system varies from one location to another. This project focuses on the design and development of the geothermal air conditioning test rig. The Taguchi technique was used in order to achieve the optimum parameters of the system. Six parameters at three different levels are considered for the analysis.L27 orthogonal array was selected. And ANNOVA concept helps in order to obtain the impact of each parameter on the performance of the system. From the calculations, pipe length of 27 m for the load of 1.755 KW was considered for the further analysis and heat transfer coefficient of 29.11 W/mK was calculated using Boelter- Dittus Equation. CFD Simulation has been carried out for different air velocities and different air inlet temperature over the pipe surface and from the results it was observed that around 14°C of temperature drop can be achieved. From the results of the geothermal air conditioning test rig it was observed that at 25 % moisture content system gives the best results and the velocity of inlet air should be between 1 to 1.5 m/s. After heating element applied to the inlet temperature drop of around 19°C was achieved. The results are further validated with simulation results.

Keywords: Geothermal air conditioner, Taguchi Technique, Orthogonal array, ANNOVA concept, Convective heat transfer coefficient, optimum length, CFD simulation, COP, ETHE test rig,

List of Figures

List of Tables

List of Abbreviations

Sr. no	Abbreviations	Acronyms
1	ETHE	Earth tube heat exchanger
2	HVAC	Heating, Ventilation and Air Conditioning
3	CAD	Computer Aided Design
4	TR	Ton of Refrigeration
5	EUT	Earth's undisturbed temperature
6	PVC	Polyvinyl chloride
7	NTU	Number of Transfer Unit
8	NV	Number of variables
9.	ANNOVA	Analysis of variance
10.	PU	Polyurethene

Nomenclature

Sr. N0	Symbol	Meaning
1	L	Optimum Length
2	m	Meters
3	KW	Kilowatt
4	m_f	Mass flow rate
5	C_{pf}	Specific Heat Capacity of fluid
6	R_{total}	Total Resistance to Heat Transfer
7	Rconv	convection resistance inside pipe
8	Rpipe	conduction resistance of pipe
9	Rg	ground resistance
10	Di	Inner diameter of the pipe
11	hconv	Convective heat transfer coefficient
12	Do	Outer diameter of the pipe
13	Kpipe	Thermal conductivity of pipe
14	Ksoil	Thermal conductivity of soil
15	NTaguchi	Minimum number of experiments required to conduct
16	NV	Number of variables

Contents

CHAPTER 1

Introduction

In India, almost 51 % of the energy is utilized for the HVAC Systems considering both residential and commercial usage as shown in fig 1.1. From this energy consumption almost 70 % to 73% of the energy is generated by the non renewable energy sources which have adverse effects on the Earth's ecosystem. The HVAC system includes Air Conditioning (Space cooling and heating), Heating and cooling equipments, water coolers and heaters. So it is important to reduce the use of such conventional energy sources by introducing renewable sources of energy.

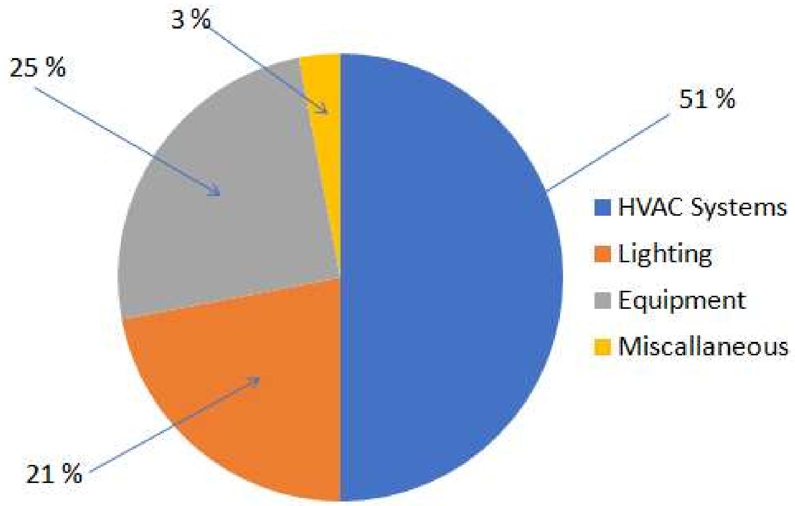

Figure no.1. 1 Pie chart of Energy consumption in India [1]

Geothermal air conditioning system is considered as a potential passive measure to reduce heating and cooling energy demand. It is composed of an array of tubes buried in the ground at a certain depth, through which atmospheric air is passed using an air blower. At around 1.5 to 2 meters, the ground temperature remains stable irrespective of the ambient temperature. This stable temperature is also called as Earth's Undisturbed Temperature. The Earth's Undisturbed Temperature (EUT) of a specific location is generally equals to the average annual temperature of that location. This property is used in geothermal air conditioning.

During the winter season when the cooled air is sent to the geothermal heat exchanger tubes, the temperature of the air increases due to heat gain from the comparatively high-temperature underground soil. This hot air is supplied to the room or the system where a heating effect is desired (Fig. 1.2(a)). Therefore, it helps in reducing the heating load of that system in winter season.

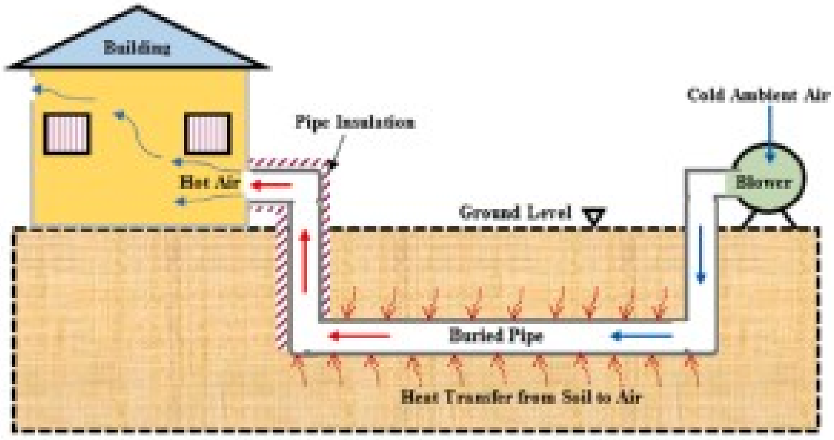

Figure no. 1.2(a) Working concept of geothermal heat exchanger system in winter season.[2]

Similarly, in summer season, cooled air can be produced using the same geothermal air conditioning system which will reduce the cooling demand (Fig. 1.2(b)). The performance of geothermal air conditioning system depends on climate condition, soil, air flow rate, dimension and material of heat exchanger tubes, and the depth at which tubes are buried in the ground. The preliminary numerical simulation was conducted on geothermal heat exchanger in ANSYS. Results revealed that for given ambient conditions and heat exchanger design parameters, temperature of ambient air can be reduced by 12 °C to 16 °C.[2].

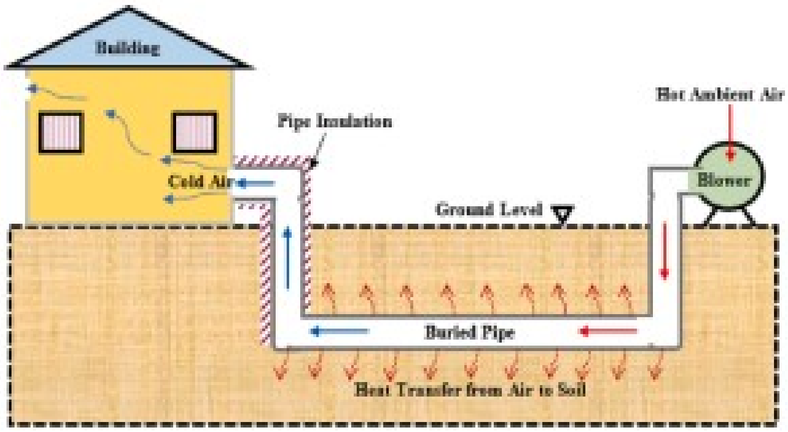

Figure no. 1.2(b) Working concept of geothermal heat exchanger system in summer season.[2]

Traditionally in order to determine optimum configuration of such systems, a numerical solution is developed, followed by an experimental setup to validate the same. In the proposed Geothermal Air Conditioning Test Rig, system parameters such as soil properties, weather conditions, dimensions and material of heat exchanger tubes and mass flow rate of air can be modulated for a scaled-down system. The test rig consists of a closely packed insulated chamber wherein environmental conditions can be controlled using air conditioning test rig. Within this insulated chamber, another chamber which is packed with soil or any backfilling material is placed along with the heat exchanger tubes at the middle of this inner chamber. The temperature of the soil at any depth in the ground near the heat exchanger tubes can be induced inside this inner chamber using controlled environment in outer chamber.

The air conditioning test rig will be helpful to induce the ambient conditions of any climatic region. This test rig will exclude the need of actual experimental setup to validate the numerical results. The inner chamber of the test rig will be designed in such a way that the heat exchanger tubes and soil or soil properties can be altered easily as per the requirement of experiment. So the with the help of this test rig, it is possible to test the probable outcomes of the outlet air temperatures considering different environmental conditions as well as the different soil properties and tube materials.

With the development of such test rig, time, cost and space required in experimental validation of the numerically simulated optimum design of geothermal heat exchanger can be reduced significantly. Year wide experimental simulation can be conducted in a short span of time. This test rig can be utilized in academic laboratories as well as for future developments of geothermal systems.

1.1.Problem Statement:

The experimentally validated design of such a system cannot be generalized for new geographical locations, as the system performance may vary significantly due to its dependency on weather and soil conditions. Significant time and financial assistance are required for new experimental results. However, they are essential to perform and validate the numerically simulated results for any variation in design parameters.

So the Problem statement is:

<u>“Design and Development of Geothermal air conditioning test rig”</u>

1.2. Objectives:

The objectives of the work to be carried out are:

1. To design and develop the Geothermal Air Conditioning Test Rig in order to reduce the cost of experimentation for different geographical locations.
2. To analyze the performance of the system by varying the soil moisture content and velocity of air in order obtain the ideal amount of each parameter.
3. To validate the numerically simulated results with the test rig results.

1.3. Methodology:

The methodology of the below project involves the following steps:

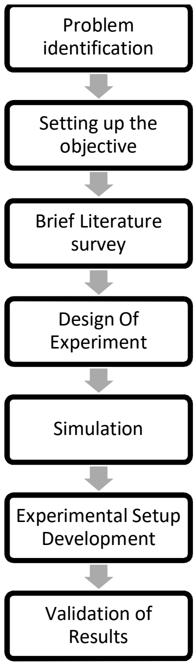

Figure no 1.3 Methodology of the project

The above methodology involves the following terms:

- Problem identification: In order to reduce the use of conventional energy sources like fossil fuels it is important introduce the systems that will work on renewable energy sources in order to reduce the dependency on the conventional sources.
- Objectives: To develop a scaled down system in order to reduce the cost of experimentation and the environmental conditions should be modulated inside the system.
- Literature survey: The most important parameter of the research is literature survey in order to get information about the previous studies.
- Design of Experiment is beneficial in achieving the impact of individual parameters on the performance of the system and by changing the parameters how the performance varies can also be identified.
- Simulation of the system using software like ANSYS is important in order to achieve the idea about the system behaviour.
- After developing the setup it is important to validate the results with the simulation results and the percentage of error between the results should be lesser.

Chapter 2

Literature Survey

2.1. Introduction

This section focuses on the prior work done by various researchers in design and development of geothermal heat exchanger. Various methods are used for design calculations and at different weather conditions for various applications have been discussed.

2.2. Previous Studies

Farheen Bano et.al [1] has examined the role of building envelop for energy efficiency in office building in India. In this paper the author has carried out the study for total amount of energy consumption from all the system including HVAC system, lighting system, equipment load and miscellaneous load for both commercial as well as residential applications and also the author has elaborated the sources of power generations for all the applications. From the study it was observed that maximum of 51 % of the total energy is consumed by the HVAC systems.

Agrawal et al. [2] presented a summary of literature indicating the performance of geothermal heat exchanger with various design strategies for piping/tubing such as piping layout, material and dimensions of the pipe, depth and slope of the piping system. All these factors need to be considered while designing such systems. From the results it was concluded that, Ring pipe was cost effective because it saves the cost of excavation. Spiral pipes should be used where less space is available whereas grid pipe layout was most suitable for large space region. Pipe diameter should not be very high or less (Should be between 0.1 m to 0.3 m). The pipes are generally arranged in series in order to avoid the space issue.

Agrawal et al. [3] analyzed the impact of soil properties on the performance of geothermal heat exchanger system. In this investigation, secondary soil with variable thermal conductivities was used as backfilling material near the pipe area. Using the CFD simulation, it was concluded that backfilling material increases the rate of heat transfer. Therefore, the piping length requirement and hence initial cost of the system can be reduced significantly using suitable secondary soil. The use of secondary soil reduces the cost of the system only when it is used for larger period of time. Using the CFD simulation, it was concluded that backfilling material increases the rate of heat transfer. Therefore, the piping length requirement and hence initial cost of the system can be reduced up to 30% using suitable secondary soil.

Mishra et al. [4] evaluated the impact of operating duration and soil properties on the performance of geothermal air heat exchangers when used in the winter season for hot and dry climate conditions. Using the transient simulation and actual experimentation, it was observed that performance derating depends on the duration of usage, pipe length as well conductivity of the soil. Thermal performance of EATHE is greatly affected in transient operating conditions. However, the total air temperature rise under transient conditions reduced from 19.4 to 17.2◦C after 24 hrs of continuous operation for soil thermal conductivity of 0.52W/mK. Value of the same for SL2 and SL3 reduced from 19.6 to 19.2◦C and 19.6 to 19.5◦C, respectively

Singh et al. [5] conducted an experimental study on the geothermal heat exchanger for hot-dry and hot-humid ambient conditions. Concrete pipes were used in the setup and the results were compared with previous studies. Experimental investigation showed the cooling effect produced by the system varies with the depth of pipe installation and the air velocity in the pipe. Experimental investigation showed the cooling effect produced by the system varies with the depth of pipe installation and the air velocity in the pipe.

Pandey et al. [6] used Taguchi method to determine the optimum design parameters for a geothermal heat exchanger where both heating and cooling energy load is required to be reduced. In this method, eight parameters at three levels were analyzed. Results showed that diameter and thermal conductivity of the pipe are the major factors for vertical as well as horizontal piping based geothermal heat exchanger. The results showed that diameter and thermal conductivity of the pipe are the major factors for vertical as well as horizontal piping based geothermal heat exchanger.

D'Agostino et al. [7] carried the numerical investigation geothermal air heat exchanger and air-to-air heat exchangers in terms of energetic, economic, and environmental aspects for office buildings located in Italy. It was observed that the thermal energy performances of the air-to-air heat exchanger are better in winter while that of geothermal air heat exchanger is more suitable in summer. Therefore, they coupled both exchangers to utilize them in winter well as in summer condition which save the energy by about 75% to 60%. Author also reported the reduction in CO2 emissions and discounted payback in the paper.

Benrachi et al. [8] carried a numerical study on geothermal air heat exchanger and estimated its thermal performance for spiral-shaped configuration for summer cooling in Algeria. It was observed that the air temperature decreases with increasing the length of pipe. It was also found that system efficiency and COP decreased from 60 % to 33 % and 2.84 to 0.46 when air velocity increased from 2 to 5 m/s.

Fard et al. [9] studied the effect of various parameters, depth, pipe length, air velocity, and pipe material on the performance of geothermal air heat exchanger in the north-east of Iran. The effective depth of the pipe over the ground surface should be between 1.5 m to 3 m. The air velocity should be minimum in order to achieve better heat transfer. Material of the pipe should posses high thermal conductivity.

Lin et al. [10] studied the impact of soil moisture content and soil thermal properties on the thermal performance of the geothermal air heat exchanger. Experimental setup was developed at University of Strasbourg. Author proposed the analytical solution based on thermal properties of different soil layers. Numerical investigation was carried out by considering different soil saturation conditions. About 40% of enhancement in the system performance was observed when fully developed flow was developed in the turbulence flow at 4 m/s.

Amanowicz and Wojtkowiak [11] evaluated the energy gains and electricity consumption of single and multipipe geothermal air heat exchanger in the for large-volume buildings. Experimental investigation on pressure losses in three, five, and seven pipes used on geothermal air heat exchangers were carried out. It was found that the thermal performance in multi pipe can be improved by using larger diameter pipes.

W. Morshed et.al (2019) [12] carried out an experimental study on heating performance of the earth air heat exchanger of tubular PVC pipe applied to a greenhouse in the costal area of west Syria. The pipe used in the heat exchanger having 20 m length and was buried at a depth of 1m. The two pipes were used having diameters of 10.16 cm and 15.24 cm each with the velocities of 1.5 and 2 m/s respectively. This method is generally beneficial in improving the crops life as well as an economical source of air conditioning. The tests were performed in the month of

December 2020. In the winter period the increase in heating performance was obtained which was about 56% for 10.16cm diameter and 36.28% for 15.24 cm diameter respectively. So from these results it was concluded that the smaller diameter tube will provide better performance than the larger one and with decrease in the air flow velocity the temperature was supposed to be increased upto 6.99 °c.

N sakhri et.al (2021) [13] investigated the impact of the environmental conditions on the efficiency of earth to air heat exchanger by experimenting four cases 1) simple EAHE 2) Earth air heat exchanger with solar protection 3) EAHE with chimney effect at the outlet 4) An EAHE with fan at the inlet and from experimentation relative humidity and air temperature at the inlet and outlet were obtained. The PVC tubes buried at a distance of 1500 mm with 2 mm thickness, 60 m horizontal length, 110 mm pipe diameter and thermal conductivity of 0.2 W/mK were selected for all the cases and From the results it was observed that the EAHE with fan at the inlet gives better performance i.e temperature difference in this case was 12.5°c and reduced environmental impact was observed in this case but this case showed some drying tendency with decrease in change in relative humidity by almost 30%.

Deldan Namgial et.al [14] investigated the performance of thermo hydraulic single pass earth air heat exchanger by experimentation and by design method of paepe and janssens. The experimentation was carried out in Punjab agricultural University, Ludhiana, india. The temperature sensors and D12 data loggers were used for data recording. The tube efficiencies of earth air heat exchanger are calculated at the velocities of 2.3, 3, 6, 11, 14 and 24 m/s. And the maximum mean tube efficiency was 64.9% and was obtained at the velocity of 2.3m/s. The designed pipe of diameter 0.25 m was at tube efficiency of 65% and velocity of 6.08 m/s. So from the results the observed average tube efficiency was found to 47.1% with the velocity of 6m/s. And it was also observed that with the increase in velocity the efficiency of the EAHE found to be decreased.

Trilok Bisoniya [15] in Design of earth - air heat exchanger system has developed a 1 dimensional mathematical model of earth air heat exchanger system with the help of some design equation. To obtain the higher accuracy in the calculation the author has calculated the nusselt number, friction factor and the Earth's undisturbed temperature (EUT). The equations developed by the author were helpful in calculating the heat transfer, convective heat transfer coefficient, length of the pipe and drop in the pressure. To simplify the model the author has made some assumptions like inlet temperature of air is equal to the ground surface temperature and also equal with the outside air temperature. Thickness of the pipe was too small hence thermal resistance of the pipe material was considered as negligible. Author also considered some boundary conditions to further simplify the problem. For the heat transfer rate calculation Number of transfer units (NTU) method was used. In the paper PVC pipe was used with the burial length of 19.228m and inner diameter of the pipe was 0.1016m. The EUT value was calculated as 25.2°c. In this paper performance of EAHE was measured by considering air velocities of 2, 3.5, 5 m/s. From the results it was concluded that the pipe with longer length and small diameter as well as the low air velocity enhances the performance of EAHE system.

Anand Kumar Patel et.al [16] investigated Geothermal heat exchanger at different orientation by using CFD analysis. The objective of this work was to analyze the performance of earth tube heat exchanger for different designs like horizontal pipes, vertical pipes and inclined pipes in summer as well as winter season with air velocities of 0.5, 1, 2, 3, 4, 5 m/s. The system uses passive renewable energy to produce heat transfer effect. The mathematical model of the system is created by using governing equations. Then after creating the geometry the input conditions and other parameters are applied in the Ansys fluent software and temperature distribution, velocity distribution and pressure distribution for each case was calculated. And from the results it was observed that earth tube heat exchanger using horizontal pipes gives better results than other two arrangements. So the heat exchanger with horizontal pipes was recommended for better thermal comfort.

Kamal Kumar Agarwal et.al [17] has evaluated the feasibility of backfilling materials for ground air heat exchanger system by using CFD simulation. In this paper the author stated that the cost of the GAHE is high due to the requirement of the larger pipes so to reduce the length of pipe some secondary soil with higher thermal conductivity were used and identified the feasibility of using backfilling materials in the vicinity of the GAHE pipe. Simulation of this system was done using Ansys fluent. In this paper author compared the performance of the four different materials like dry native soil, wet native soil, dry sand bentonite mixture, wet sand bentonite mixture which were considered as backfilling materials. From the cost analysis it was clearly understood that the initial cost with wet sand bentonite, dry sand bentonite and wet native soil as backfilling materials were approximately 17.9%, 20.7% and 30% respectively, lesser than the GAHE with ordinary soil or the dry native soil as backfilling material. And for all these four BFMs the temperature difference were also calculated by using both analytical and simulation method for various pipe lengths as well as the time taken by the system and it was observed that after 1 hr for 60 m length pipe the difference was 6.1% and similarly after 6h the difference between both analytical and simulation results were found to be 6.4%.

Nikhil Jagtap et.al (2018) [18] has evaluated an implicit model based on transient analysis using computational fluid dynamics is developed to predict the performance of heat exchanger and also the capability of the earth tube heat exchanger. The author has developed the mathematical model of the system by using the software MATLAB for validation of results and comparative analysis. The output temperature is measure of effectiveness of this system, affected majorly by the inner radius of heat exchanger, its thickness, the conductivity of material, length of pipe and depth at which the heat exchanger is laid.

Paepe et.al (2003) [19] has investigated one dimensional analytical method to analyze the influence of the operating parameters on the performance of earth tube heat exchanger. A relation derived for specific pressure drop, linking thermal effectiveness for the pressure drop of the air inside the tube. So this system allows the designer to select the earth tube heat exchanger depending on the best performance of the system.

The constructor [20] site gives the detailed idea about how to carry out the core cutter test and from the soil sample it is possible to calculate the moisture content present in the soil and the density of the soil i.e. bulk density and field density. The website has elaborated the step by step procedure for the core cutter test.

2.3. Summary of Literature

The extensive literature showed that the research work in the domain of geothermal heat exchanger is based on numerical analysis followed by actual experimental investigation. The outcomes of experimental procedures depend on site-specific parameters such as weather conditions and soil properties. These two parameters also vary with time. Therefore, even the experimentally validated design of such a system cannot be generalized for new geographical locations, as the system performance may vary significantly due to its dependency on weather and soil conditions. Significant time and financial assistance are required for new experimental results. However, they are essential to perform to validate the numerically simulated results for any variation in design parameters. Some important factors should be considered from the literature study are: The diameter of pipe should be between 0.1m to 0.3 m (Agrawal et al.). Horizontal pipe gives better performance than vertical pipes (Pandey et al.) Velocity should be minimum in order to achieve higher heat transfer rate (Morshed et al.). Better performance can be achieved with multi pipe arrangement (Namgial,). Minimum thickness of pipe can enhance the heat transfer effect (Jagtap et al.) Impact of moisture content might be significant (Bisoniya) These factors should be considered while developing the system.

Chapter -3

Design of Experiment

3.1. Cooling Load Estimation:

For the Geothermal air conditioning test rig, it is important to obtain the optimum values of the controlling parameters.

- To calculate the optimum length of geothermal air conditioner several volumes of different sizes were considered.
- The Cooling load inside the volume was estimated by using relation,

  Cooling Load (KW) = U× A × ΔT
- The cooling load inside the volume was calculated by considering both sensible and latent loads (Number of occupants, electronic devices, infiltration, glass types, heat gain through wall and windows etc.)
- Considering the volume of size 171.26 m^3, the total load estimated comprises of sensible load, latent load and losses. The individual load can be estimated by substituting the given values in the above equation of cooling load.

  Sensible heat load comprises of:

  - Solar heat gain through windows= 0.33 KW
  - Solar heat gain through wall= 0.36 KW
  - Heat transmission from wall and glass= 1.33 KW
  - Internal heat gain by occupants (considering 7 occupants) = 0.42 KW.
  - Electrical and computer equipment load= 0.53 KW.
  - Lighting load= 0.33 KW.
  - The sensible load with 12.5 % of losses= 0.41 KW.
  - Total sensible load including the losses= 3.71 KW.

  Latent heat load comprises of:
  - Latent load from occupants= 0.50 KW
  - 10 % latent load losses= 0.050 KW.
  - Total latent load= 0.55 KW.

  Outdoor air heat load:
  - Outdoor air sensible heat load= 0.38 KW.
  - Outdoor air latent heat load= 0.85 KW.

  Therefore the total cooling load can be estimated from the summation of all the loads:
  Total cooling load= Sensible load + latent load + OASH + OALH

Total cooling load= 5.51.KW.

Therefore after adding the sensible, latent and outdoor air load, the value of cooling load for the volume of size 171.26 m3 can be achieved as 5.51 KW. Similar method was used to calculate the cooling load for the remaining volumes.

- From the cooling loads, the mass flow rate, velocity of air and optimum length of the pipe was estimated for both space heating and space cooling.
- The below table shows the volumes and the load inside it.

Table no 3.1. Cooling load table

Volume size (m3)	Cooling Load (KW)
1.78	0.14
4.23	0.23
8.46	0.4
34.13	1.5
56.45	2.49
108.8	3.42
139.8	4.3
171.26	5.51

3.2. Governing equations for horizontal ground heat exchanger

Thermodynamic modeling of ground heat exchanger

3.2.1. Space cooling: heat rejection into the ground

For a steady flow process, the governing equations are obtained based on mass and energy conservation principles. Following governing equations have been utilized for the design of horizontal ground heat exchanger

For space cooling:

The length of pipe can be estimated by the relation:

Heat rejection into the ground = heat transfer from the heat exchange pipe.[6]

$$dq = -m_{f\times} C_{f\times} dT_f = \left[\frac{(T_{fx} - T_g)}{R_{total}}\right] dx \quad (1)$$

$$\frac{\theta_f}{\theta_{fin}} = e^{\left[\frac{-x}{m_{f\times} C_f \times R_{Total}}\right]} \quad (2)$$

Length of ground air conditioner $L = m_{f\times} C_{pf} \times R_{Total} \times \ln \frac{\theta_{fin}}{\theta_{fout}}$ (3)

Where,

m_f = mass flow rate (kg/s)

C_{pf} = Specific heat capacity of fluid (J/kg K)

R_{total} = Total resistance to heat transfer (m K/W)

$$\theta_{fin} = (T_{fin} - T_g) \quad (4)$$
$$\theta_{fout} = (T_{fout} - T_g) \quad (5)$$

T_{fin} = Temperature of Fluid at inlet (K)

T_{fout}= Temperature of Fluid at Outlet (K)

T_g = Temperature of ground (K)

$$R_{total} = R_{conv} + R_{pipe} + R_g \quad (6)$$

R_{conv}=convection resistance inside pipe (m K/W)

R_{pipe} = conduction resistance of pipe (m K/W)

R_g= ground resistance (m K/W)

$$Rconv = \frac{1}{(\pi Dih_{conv})}, Rpipe = In\left\{\frac{\frac{Do}{Di}}{(2\pi k_{pipe})}\right\},\ Rg = \frac{1}{K_{soil}} \quad (7)$$

Where,

Di = Inner diameter of the pipe (m)

hconv = Convective heat transfer coefficient (W/m2 K)

Do = Outer diameter of the pipe (m)

Kpipe = Thermal conductivity of pipe (W/m K)

Ksoil = Thermal conductivity of soil (W/m K)

3.2.2. For Space heating:

Space Heating: Heat extraction from the ground

Heat extraction from the ground = heat transfer from the heat exchange pipe

$$L = m_{f\times} C_{pf} \times R_{Total} \times \ln\frac{\theta_{fout}}{\theta_{fin}} \quad (8)$$

Where,

L= Optimum length required for space heating (m).

The value of convective heat transfer coefficient inside and outside of the pipe is calculated by using Dittus-Boelter equation.[16]

$Nu = 0.023 \times (Re)^{0.8} \times Pr^{n}$ (9)

hi. Di / K_a= $0.023 \times (Re)^{0.8} \times Pr^{n}$ (10)

The value of n is considered as 0.4.

Nu= Nusselt Number

hi= convective heat transfer coefficient inside of the pipe.

ho= convective heat transfer coefficient outside of the pipe.

And,

ho = 5.7 + 3.8V (11)

(where v= velocity of air)

3.3. Taguchi Technique:

Taguchi optimization is an experimental technique that suggests the matrix of experiments by using standard orthogonal arrays (OA).With the help of this matrix, maximum information from minimum number of experiments and also the best level of each parameter can be obtained. Signal-to-noise (S/N) ratios are used to calculate the response of the experimental trials. As the objective of this study is to obtain the minimum length that can give the optimum results hence lower the better function is selected. Analysis of variance (ANNOVA) helps in obtaining the impact of individual parameter.

For performing the Taguchi optimization six parameters at three levels have been considered. The factors which are considered are: Thermal conductivity of pipe (W/mK), Diameter of pipe (m), Depth from the ground (m), Air inlet temperature (K), Velocity of air (m/s), Mass flow rate of air (kg/s).

As six factors at three different levels are considered so the minimum number of experiments to be conducted can be preset by the below relation:[6]

$$N_{Tag} \quad = 1 + NV(L-1) \tag{12}$$

Where,

$N_{Taguchi}$ = Minimum number of experiments required to conduct

NV = Number of variables or control parameters

L = Number of levels selected.

So the nearest orthogonal array is selected is L27 Orthogonal array for the Experimental trials.

The S/N ratio by considering lower the better function can be calculated by using following equation:

$$Lower\ the\ better\ S/N(dB) = -10\ \log\left(\frac{1}{n}\sum_{i=1}^{n} Yi^{\,2}\right) \tag{13}$$

Where,

Yi = Performance value of the observation

n= Number of repetitions in a trial.

3.4. Analysis of Variance (ANNOVA):

Analysis of variance (ANNOVA) helps in obtaining the impact of individual parameter.

Following formulae have been used to calculate the sum of squares (SS), variance, Degrees of Freedom and Percentage of contribution:

$$SS = \left\{(Sum\ of\ \frac{S}{N}ratio\ level\ 1)^2 + (Sum\ of\ \frac{S}{N}ratio\ level\ 2)^2 + (Sum\ of\ \frac{S}{N}ratio\ level\ 3)^2 - CF\right\} \tag{14}$$

$$Correction\ facrtor\ C.F. = \frac{\left(Sum\ of\ \frac{S}{N}\right)^2}{N} \tag{15}$$

Where N is the total number of Experiments (N=27)

Degree of freedom= Level-1

$$Variance = \frac{(SS)}{DOF} \qquad (16)$$

$$Percentage\ contribution = \frac{(SS\ of\ individual\ factor \times 100)}{\sum_{i=1}^{n} SS} \qquad (17)$$

$$F - Ratio = \frac{(Mean\ square\ of\ a\ factor)}{Mean\ square\ error} \qquad (18)$$

3.5. Control Factors and Their levels:

So for the cooling load of 5.51 KW,

Control factors and their level of geothermal air conditioner for space cooling and heating will be:

Table No 3.2. Control Factors and their levels for space cooling (Load=5.51 KW)

Factors	Parameters	Level		
		1	2	3
A	Thermal conductivity of pipe (W/mK)	0.16	0.26	0.36
B	Diameter of pipe (m)	0.08	0.09	0.1
C	Depth from the ground (m)	1.5	2	2.5
D	Air inlet Temperature (K)	312	313	314
E	Velocity of air (m/s)	4.2	4.25	4.3
F	Mass flow rate of air (Kg/s)	0.05	0.055	0.06

Table No 3.3. Control Factors and their levels for space heating (Load=5.51 KW)

Factors	Parameters	Level		
		1	2	3
A	Thermal conductivity of pipe (W/mK)	0.16	0.26	0.36
B	Diameter of pipe (m)	0.08	0.09	0.1
C	Depth from the ground (m)	1.5	2	2.5
D	Air inlet Temperature (K)	289	290	291

E	Velocity of air (m/s)	4.2	4.25	4.3
F	Mass flow rate of air (Kg/s)	0.05	0.055	0.06

3.6. Orthogonal arrays:

Now once the above control factors and their levels are substituted in the L27 Orthogonal array then the matrix will look like

Table No. 3.4. L27 Orthogonal matrix for 5.51 KW load values

Sr. No	Thermal conductivity of pipe (W/mK)	Diameter of pipe (m)	Depth from the ground (m)	Air inlet Temperature (K)	Velocity of air (m/s)	Mass flow rate of air (Kg/s)
1	0.16	0.08	1.5	312	4.2	0.345
2	0.16	0.08	1.5	312	4.25	0.355
3	0.16	0.08	1.5	312	4.3	0.365
4	0.16	0.09	2	313	4.2	0.345
5	0.16	0.09	2	313	4.25	0.355
6	0.16	0.09	2	313	4.3	0.365
7	0.16	0.1	2.5	314	4.2	0.345
8	0.16	0.1	2.5	314	4.25	0.355
9	0.16	0.1	2.5	314	4.3	0.365
10	0.26	0.08	2	314	4.2	0.355
11	0.26	0.08	2	314	4.25	0.365
12	0.26	0.08	2	314	4.3	0.345
13	0.26	0.09	2.5	312	4.2	0.355
14	0.26	0.09	2.5	312	4.25	0.365
15	0.26	0.09	2.5	312	4.3	0.345

16	0.26	0.1	1.5	313	4.2	0.355
17	0.26	0.1	1.5	313	4.25	0.365
18	0.26	0.1	1.5	313	4.3	0.345
19	0.36	0.08	2.5	313	4.2	0.365
20	0.36	0.08	2.5	313	4.25	0.345
21	0.36	0.08	2.5	313	4.3	0.355
22	0.36	0.09	1.5	314	4.2	0.365
23	0.36	0.09	1.5	314	4.25	0.345
24	0.36	0.09	1.5	314	4.3	0.355
25	0.36	0.1	2	312	4.2	0.366
26	0.36	0.1	2	312	4.25	0.345
27	0.36	0.1	2	312	4.3	0.355

After substituting all the values of the factors and their levels in the formula's mentioned in the earlier pages, we get the length of pipe and S/N ratios for all the experiments

Table No. 3.5. L27 Orthogonal matrix for 5.51 KW load with cooling length & S/N Ratio's.

Sr. No	Thermal conductivity of pipe (W/mK)	Diameter of pipe (m)	Depth from the ground (m)	Air inlet Temperature (K)	Velocity of air (m/s)	Mass flow rate of air (Kg/s)	Space cooling length (m)	S/N ratio for Cooling
1	0.16	0.08	1.5	312	4.2	0.345	230.0632969	-47.23694678
2	0.16	0.08	1.5	312	4.25	0.355	253.0696266	-48.06480049
3	0.16	0.08	1.5	312	4.3	0.365	276.0759563	-48.8205717
4	0.16	0.09	2	313	4.2	0.345	232.153614	-47.31550898

5	0.16	0.09	2	313	4.25	0.355	255.3689754	-48.14336268
6	0.16	0.09	2	313	4.3	0.365	278.5843368	-48.8991339
7	0.16	0.1	2.5	314	4.2	0.345	212.05474	-46.52895969
8	0.16	0.1	2.5	314	4.25	0.355	233.260214	-47.35681339
9	0.16	0.1	2.5	314	4.3	0.365	254.465688	-48.11258461
10	0.26	0.08	2	314	4.2	0.355	210.763036	-46.47588892
11	0.26	0.08	2	314	4.25	0.365	229.923312	-47.23166014
12	0.26	0.08	2	314	4.3	0.345	191.60276	-45.64803521
13	0.26	0.09	2.5	312	4.2	0.355	192.8680414	-45.7052054
14	0.26	0.09	2.5	312	4.25	0.365	210.4014997	-46.46097662
15	0.26	0.09	2.5	312	4.3	0.345	175.3345831	-44.8773517
16	0.26	0.1	1.5	313	4.2	0.355	171.3962943	-44.68002856
17	0.26	0.1	1.5	313	4.25	0.365	186.9777756	-45.43579978
18	0.26	0.1	1.5	313	4.3	0.345	155.814813	-43.85217486
19	0.36	0.08	2.5	313	4.2	0.365	183.2131224	-45.25913152
20	0.36	0.08	2.5	313	4.25	0.345	152.677602	-43.6755066
21	0.36	0.08	2.5	313	4.3	0.355	167.9453622	-44.50336031
22	0.36	0.09	1.5	314	4.2	0.365	180.83856	-45.1458208
23	0.36	0.09	1.5	314	4.25	0.345	150.6988	-43.56219588

24	0.36	0.09	1.5	314	4.3	0.355	165.76868	-44.39004958
25	0.36	0.1	2	312	4.2	0.366	141.0784622	-42.98921434
26	0.36	0.1	2	312	4.25	0.345	117.5653852	-41.40558942
27	0.36	0.1	2	312	4.3	0.355	129.3219237	-42.23344313

Table No. 3.6. L27 Orthogonal matrix for 5.51 KW load with Heating length & S/N Ratio's

Sr. No	**Thermal conductivity of pipe (W/mK)**	**Diameter of pipe (m)**	**Depth from the ground (m)**	**Air inlet Temperature (K)**	**Velocity of air (m/s)**	**Mass flow rate of air (Kg/s)**	**space heating length (m)**	**S/N ratio for heating**
1	0.16	0.08	1.5	289	4.2	0.345	237.382299	-47.50896663
2	0.16	0.08	1.5	289	4.25	0.355	261.1205289	-48.33682033
3	0.16	0.08	1.5	289	4.3	0.365	284.8587588	-49.09259155
4	0.16	0.09	2	290	4.2	0.345	217.2908694	-46.74082955
5	0.16	0.09	2	290	4.25	0.355	239.0199563	-47.56868325
6	0.16	0.09	2	290	4.3	0.365	260.7490433	-48.32445447
7	0.16	0.1	2.5	291	4.2	0.345	177.37289	-44.97774484
8	0.16	0.1	2.5	291	4.25	0.355	195.110179	-45.80559855
9	0.16	0.1	2.5	291	4.3	0.365	212.847468	-46.56136976
10	0.26	0.08	2	291	4.2	0.355	176.292446	-44.92467407
11	0.26	0.08	2	291	4.25	0.365	192.319032	-45.68044529

12	0.26	0.08	2	291	4.3	0.345	160.26586	-44.09682037
13	0.26	0.09	2.5	289	4.2	0.355	199.0037511	-45.97722525
14	0.26	0.09	2.5	289	4.25	0.365	217.0950012	-46.73299647
15	0.26	0.09	2.5	289	4.3	0.345	180.912501	-45.14937155
16	0.26	0.1	1.5	290	4.2	0.355	160.423304	-44.10534913
17	0.26	0.1	1.5	290	4.25	0.365	175.0072408	-44.86112035
18	0.26	0.1	1.5	290	4.3	0.345	145.8393673	-43.27749543
19	0.36	0.08	2.5	290	4.2	0.365	171.483605	-44.6844521
20	0.36	0.08	2.5	290	4.25	0.345	142.9030042	-43.10082718
21	0.36	0.08	2.5	290	4.3	0.355	157.1933046	-43.92868088
22	0.36	0.09	1.5	291	4.2	0.365	151.26216	-43.59460596
23	0.36	0.09	1.5	291	4.25	0.345	126.0518	-42.01098103
24	0.36	0.09	1.5	291	4.3	0.355	138.65698	-42.83883474
25	0.36	0.1	2	289	4.2	0.366	140.0352	-42.92474432
26	0.36	0.1	2	289	4.25	0.345	116.696	-41.3411194
27	0.36	0.1	2	289	4.3	0.355	128.3656	-42.1689731

The above table shows the required length of cooling and heating with their S/N ratios of all the 27 orthogonal arrays.

3.7. Response Table for signal to noise ratio

3.7.1. Response Table for signal to noise ratio (cooling load= 5.51 KW)

From the Taguchi L27 Orthogonal array the response table for Signal to noise ratio for the Cooling load of 5.51 KW is obtained for both space heating and cooling.

Table no 3.7. Response Table for signal to noise ratio for space Cooling

Level	Thermal conductivity of pipe (W/mK)	Diameter of pipe (m)	Depth from the ground (m)	Air inlet Temperature (K)	Velocity of air (m/s)	Mass flow rate of air (Kg/s)
1	-47.83	-46.32	-45.69	-45.31	-45.70	-44.90
2	-45.60	-46.06	-45.59	-45.75	-45.70	-45.73
3	-43.68	-44.73	-45.83	-46.05	-45.70	-46.48
Delta	4.15	1.59	0.24	0.74	0.00	1.58
Rank	1	2	5	4	6	3

Table no 3.8. Response Table for signal to noise ratio for space Heating

Level	Thermal conductivity of pipe (W/mK)	Diameter of pipe (m)	Depth from the ground (m)	Air inlet Temperature (K)	Velocity of air (m/s)	Mass flow rate of air (Kg/s)
1	-47.21	-45.71	-45.07	-45.47	-45.05	-44.24
2	-44.98	-45.44	-44.86	-45.18	-45.05	-45.07
3	-42.95	-44.00	-45.21	-44.50	-45.05	-45.83
Delta	4.26	1.70	0.35	0.97	0.00	1.58
Rank	1	2	5	4	6	3

As the minimum length will be the optimum value of the length hence lower the better concept is selected. So for that minimum value of the S/N ratio for each parameter i.e. table 3.7. and table 3.8. will be considered as the optimum value of that parameter at that level.

And the values of optimum parameters is substituted in the Optimum space cooling and heating formula and the final value of the optimum length is obtained about 117 m for space cooling and 116 m for space heating.

In similar way all the orthogonal arrays are solved for their respective cooling loads and the ratio of their signal to noise ratios are given in the below tables.

3.7.2. Response Table for signal to noise ratio (cooling load= 4.3 KW)

Previously the volume of the space selected for conditioning was too large and so to minimize the length of the pipe, the volume of the space to be conditioned was reduced in order to achieve the Optimum length. And as the Volume decreases the cooling load inside the space also reduces.

So the Response table for signal to noise ratio has been evaluated for both space heating as well as cooling.

For the load of 4.3 KW, the Signal to noise ratio will be

Table no 3.9. Response Table for signal to noise ratio for space Cooling

Level	Thermal conductivity of pipe (W/mK)	Diameter of pipe (m)	Depth from the ground (m)	Air inlet Temperature (K)	Velocity of air (m/s)	Mass flow rate of air (Kg/s)
1	-46.08	-44.57	-43.93	-43.56	-43.95	-42.96
2	-43.84	-44.30	-43.84	-44.00	-43.95	-43.99
3	-41.93	-42.98	-44.08	-44.30	-43.95	-44.90
Delta	4.15	1.59	0.24	0.74	0.00	1.94
Rank	1	3	5	4	6	2

Table no 3.10. Response Table for signal to noise ratio for space Heating

Level	Thermal conductivity of pipe (W/mK)	Diameter of pipe (m)	Depth from the ground (m)	Air inlet Temperature (K)	Velocity of air (m/s)	Mass flow rate of air (Kg/s)
1	-45.46	-43.95	-43.31	-43.72	-43.29	-42.31
2	-43.22	-43.68	-43.11	-43.42	-43.29	-43.33
3	-41.20	-42.25	-43.46	-42.74	-43.29	-44.24
Delta	4.26	1.70	0.35	0.97	0.00	1.94
Rank	1	3	5	4	6	2

As the minimum length will be the optimum value of the length hence lower the better concept is selected. So for that minimum value of the S/N ratio for each parameter i.e. table 3.9. And table 3.10.will be considered as the optimum value of that parameter at that level. The optimum values are (A3,B3,C1,D1,E1,F1) for space cooling and (A3,B3,C1,D3,E1,F1) for space heating.

3.7.3. Response Table for signal to noise ratio (cooling load= 3.42 KW)

For the load of 3.42 KW, the Signal to noise ratio will be

Table no 3.11. Response Table for signal to noise ratio for space Cooling

Level	Thermal conductivity of pipe (W/mK)	Diameter of pipe (m)	Depth from the ground (m)	Air inlet Temperature (K)	Velocity of air (m/s)	Mass flow rate of air (Kg/s)
1	-43.87	-42.36	-41.73	-41.35	-41.74	-40.46
2	-41.63	-42.09	-41.63	-41.79	-41.74	-41.80
3	-39.72	-40.77	-41.87	-42.09	-41.74	-42.96
Delta	4.15	1.59	0.24	0.74	0.00	2.50
Rank	1	3	5	4	6	2

Table no 3.11. Response Table for signal to noise ratio for space Cooling

Level	Thermal conductivity of	Diameter of pipe (m)	Depth from the ground	Air inlet Temperature	Velocity of air (m/s)	Mass flow rate of air

	pipe (W/mK)		(m)	(K)		(Kg/s)
1	-43.25	-41.74	-41.11	-41.51	-41.09	-39.81
2	-41.02	-41.48	-40.90	-41.22	-41.09	-41.15
3	-38.99	-40.04	-41.25	-40.54	-41.09	-42.31
Delta	4.26	1.70	0.35	0.97	0.00	2.50
Rank	1	3	5	4	6	2

Table no 3.11. And table 3.12. shows the optimum values of that parameter at that level for the cooling load of 3.42 KW. The optimum values are (A3,B3,C1,D1,E1,F1) for space cooling and (A3,B3,C1,D3,E1,F1) for space heating.

3.7.4. Response Table for signal to noise ratio (cooling load= 2.49 KW)

For the load of 2.49 KW, the Signal to noise ratio will be

Table no 3.13. Response Table for signal to noise ratio for space Cooling

Level	Thermal conductivity of pipe (W/mK)	Diameter of pipe (m)	Depth from the ground (m)	Air inlet Temperature (K)	Velocity of air (m/s)	Mass flow rate of air (Kg/s)
1	-40.89	-39.38	-38.74	-38.37	-38.76	-36.94
2	-38.65	-39.11	-38.65	-38.81	-38.76	-38.88
3	-36.74	-37.79	-38.89	-39.11	-38.76	-40.46
Delta	4.15	1.59	0.24	0.74	0.00	3.52
Rank	1	3	5	4	6	2

Table no 3.14. Response Table for signal to noise ratio for space Heating

Level	Thermal conductivity of pipe (W/mK)	Diameter of pipe (m)	Depth from the ground (m)	Air inlet Temperature (K)	Velocity of air (m/s)	Mass flow rate of air (Kg/s)
1	-40.27	-38.76	-38.13	-38.53	-38.11	-36.29
2	-38.04	-38.49	-37.92	-38.23	-38.11	-38.22
3	-36.01	-37.06	-38.27	-37.56	-38.11	-39.81
Delta	4.26	1.70	0.35	0.97	0.00	3.52
Rank	1	3	5	4	6	2

Table no 3.13. and table 3.14. shows the optimum values of that parameter at that level for the cooling load of 2.49 KW. The optimum values are (A3,B3,C1,D1,E1,F1) for space cooling and (A3,B3,C1,D3,E1,F1) for space heating.

3.7.5. Response Table for signal to noise ratio (cooling load= 1.755 KW)

For the load of 1.755 KW, the Signal to noise ratio will be

Table no 3.15. Response Table for signal to noise ratio for space Cooling

Level	Thermal conductivity of pipe (W/mK)	Diameter of pipe (m)	Depth from the ground (m)	Air inlet Temperature (K)	Velocity of air (m/s)	Mass flow rate of air (Kg/s)
1	-37.03	-35.52	-34.88	-34.44	-34.88	-33.18
2	-34.79	-35.25	-34.72	-34.95	-34.88	-34.98
3	-32.82	-33.86	-35.03	-35.25	-34.88	-36.47
Delta	4.21	1.66	0.30	0.81	0.00	3.30
Rank	1	3	5	4	6	2

Table no 3.16. Response Table for signal to noise ratio for space Heating

Level	Thermal conductivity of pipe (W/mK)	Diameter of pipe (m)	Depth from the ground (m)	Air inlet Temperature (K)	Velocity of air (m/s)	Mass flow rate of air (Kg/s)
1	-36.41	-34.90	-34.27	-34.52	-34.19	-32.49
2	-34.17	-34.63	-33.91	-34.37	-34.19	-34.30
3	-32.00	-33.05	-34.41	-33.69	-34.19	-35.79
Delta	4.41	1.85	0.50	0.82	0.00	3.30
Rank	1	3	5	4	6	2

Table no 3.15. and table 3.16. shows the optimum values of that parameter at that level for the cooling load of 1.755 KW. The optimum values are (A3,B3,C1,D1,E1,F1) for space cooling and (A3,B3,C1,D3,E1,F1) for space heating.

3.7.6. Response Table for signal to noise ratio (cooling load= 1.5 KW)

For the load of 1.5 KW, the Signal to noise ratio will be

Table no 3.17. Response Table for signal to noise ratio for space Cooling

Level	Thermal conductivity of pipe (W/mK)	Diameter of pipe (m)	Depth from the ground (m)	Air inlet Temperature (K)	Velocity of air (m/s)	Mass flow rate of air (Kg/s)
1	-36.23	-34.72	-34.09	-33.71	-34.10	-30.92
2	-33.99	-34.45	-33.99	-34.15	-34.10	-34.44
3	-32.08	-33.13	-34.23	-34.45	-34.10	-36.94
Delta	4.15	1.59	0.24	0.74	0.00	6.02
Rank	2	3	5	4	6	1

Table no 3.18. Response Table for signal to noise ratio for space Heating

Level	Thermal conductivity of pipe (W/mK)	Diameter of pipe (m)	Depth from the ground (m)	Air inlet Temperature (K)	Velocity of air (m/s)	Mass flow rate of air (Kg/s)
1	-35.61	-34.10	-33.47	-33.87	-33.45	-30.27
2	-33.38	-33.84	-33.26	-33.57	-33.45	-33.79
3	-31.35	-32.40	-33.61	-32.90	-33.45	-36.29

Delta	4.26	1.70	0.35	0.97	0.00	6.02
Rank	2	3	5	4	6	1

Table no 3.17. and table 3.18. shows the optimum values of that parameter at that level for the cooling load of 1.5 KW. The optimum values are (A3,B3,C1,D1,E1,F1) for space cooling and (A3,B3,C1,D3,E1,F1) for space heating.

3.7.7. Response Table for signal to noise ratio (cooling load= 0.4 KW)

For the load of 0.4 KW, the Signal to noise ratio will be

Table no 3.19. Response Table for signal to noise ratio for space Cooling

Level	Thermal conductivity of pipe (W/mK)	Diameter of pipe (m)	Depth from the ground (m)	Air inlet Temperature (K)	Velocity of air (m/s)	Mass flow rate of air (Kg/s)
1	-30.54	-29.03	-28.39	-28.02	-28.41	-27.82
2	-28.30	-28.76	-28.30	-28.46	-28.41	-28.42
3	-26.39	-27.44	-28.54	-28.76	-28.41	-28.98
Delta	4.15	1.59	0.24	0.74	0.00	1.16
Rank	1	2	5	4	6	3

Table no 3.20. Response Table for signal to noise ratio for space Heating

Level	Thermal conductivity of pipe (W/mK)	Diameter of pipe (m)	Depth from the ground (m)	Air inlet Temperature (K)	Velocity of air (m/s)	Mass flow rate of air (Kg/s)
1	-29.92	-28.41	-27.77	-28.18	-27.75	-27.17
2	-27.68	-28.14	-27.57	-27.88	-27.75	-27.77
3	-25.66	-26.71	-27.92	-27.20	-27.75	-28.33
Delta	4.26	1.70	0.35	0.97	0.00	1.16
Rank	1	2	5	4	6	3

Table no 3.19. and table 3.20. shows the optimum values of that parameter at that level for the cooling load of 0.4 KW. The optimum values are (A3,B3,C1,D1,E1,F1) for space cooling and (A3,B3,C1,D3,E1,F1) for space heating.

3.7.8. Response Table for signal to noise ratio (cooling load= 0.23 KW)

For the load of 0.23 KW, the Signal to noise ratio will be

Table no 3.21. Response Table for signal to noise ratio for space Cooling

Level	Thermal conductivity of pipe (W/mK)	Diameter of pipe (m)	Depth from the ground (m)	Air inlet Temperature (K)	Velocity of air (m/s)	Mass flow rate of air (Kg/s)

1	-26.08	-24.57	-23.93	-23.56	-23.95	-22.96
2	-23.84	-24.30	-23.84	-24.00	-23.95	-23.99
3	-21.93	-22.98	-24.08	-24.30	-23.95	-24.90
Delta	4.15	1.59	0.24	0.74	0.00	1.94
Rank	1	3	5	4	6	2

Table no 3.22. Response Table for signal to noise ratio for space Heating

Level	Thermal conductivity of pipe (W/mK)	Diameter of pipe (m)	Depth from the ground (m)	Air inlet Temperature (K)	Velocity of air (m/s)	Mass flow rate of air (Kg/s)
1	-25.46	-23.95	-23.31	-23.72	-23.29	-22.31
2	-23.22	-23.68	-23.11	-23.42	-23.29	-23.33
3	-21.20	-22.25	-23.46	-22.74	-23.29	-24.24
Delta	4.26	1.70	0.35	0.97	0.00	1.94
Rank	1	3	5	4	6	2

Table no 3.21. and table 3.22. shows the optimum values of that parameter at that level for the cooling load of 0.23 KW. The optimum values are (A3,B3,C1,D1,E1,F1) for space cooling and (A3,B3,C1,D3,E1,F1) for space heating.

3.7.9. Response Table for signal to noise ratio (cooling load= 0.14 KW)

For the load of 0.14 KW, the Signal to noise ratio will be

Table no 3.23. Response Table for signal to noise ratio for space Cooling

Level	Thermal conductivity of pipe (W/mK)	Diameter of pipe (m)	Depth from the ground (m)	Air inlet Temperature (K)	Velocity of air (m/s)	Mass flow rate of air (Kg/s)
1	-23.87	-22.36	-21.73	-21.35	-21.74	-20.46
2	-21.63	-22.09	-21.63	-21.79	-21.74	-21.80
3	-19.72	-20.77	-21.87	-22.09	-21.74	-22.96
Delta	4.15	1.59	0.24	0.74	0.00	2.50
Rank	1	3	5	4	6	2

Table no 3.24. Response Table for signal to noise ratio for space Heating

Level	Thermal conductivity of pipe (W/mK)	Diameter of pipe (m)	Depth from the ground (m)	Air inlet Temperature (K)	Velocity of air (m/s)	Mass flow rate of air (Kg/s)
1	-23.25	-21.74	-21.11	-21.51	-21.09	-19.81
2	-21.02	-21.48	-20.90	-21.22	-21.09	-21.15
3	-18.99	-20.04	-21.25	-20.54	-21.09	-22.31
Delta	4.26	1.70	0.35	0.97	0.00	2.50
Rank	1	3	5	4	6	2

Table no 3.23. And table 3.24. shows the optimum values of that parameter at that level for the cooling load of 0.14 KW. The optimum values are (A3,B3,C1,D1,E1,F1) for space cooling and (A3,B3,C1,D3,E1,F1) for space heating.

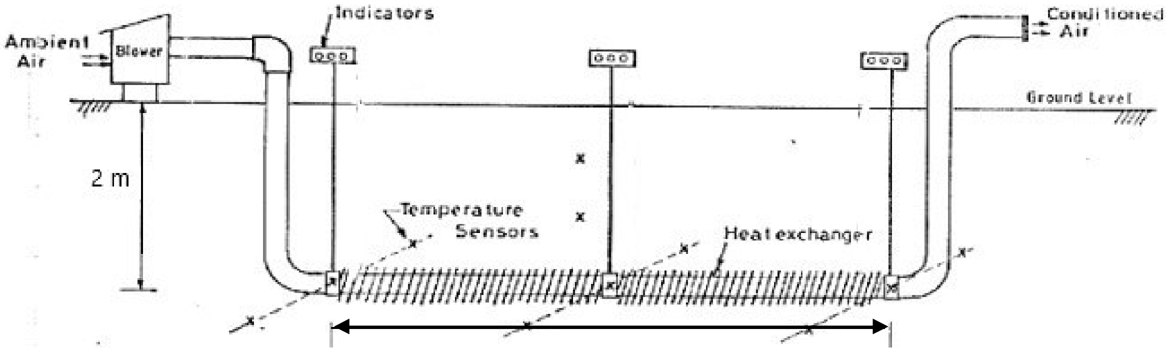

Figure no.3. 1 Optimum Length schematic

3.8. S/N Ratio Graphs:

The plots below shows that the response of each parameter at different levels.

3.8.1. S/N Ratio graphs for the Cooling load of 5.51 KW.

In the below table, K stands for Thermal conductivity of pipe (W/mK), D stands for Diameter of pipe (m), Dep stands for Depth from the ground (m), T_{in} stands for Air inlet Temperature (K), V_a stands for Velocity of air (m/s) and M_a stands for Mass flow rate of air (Kg/s).

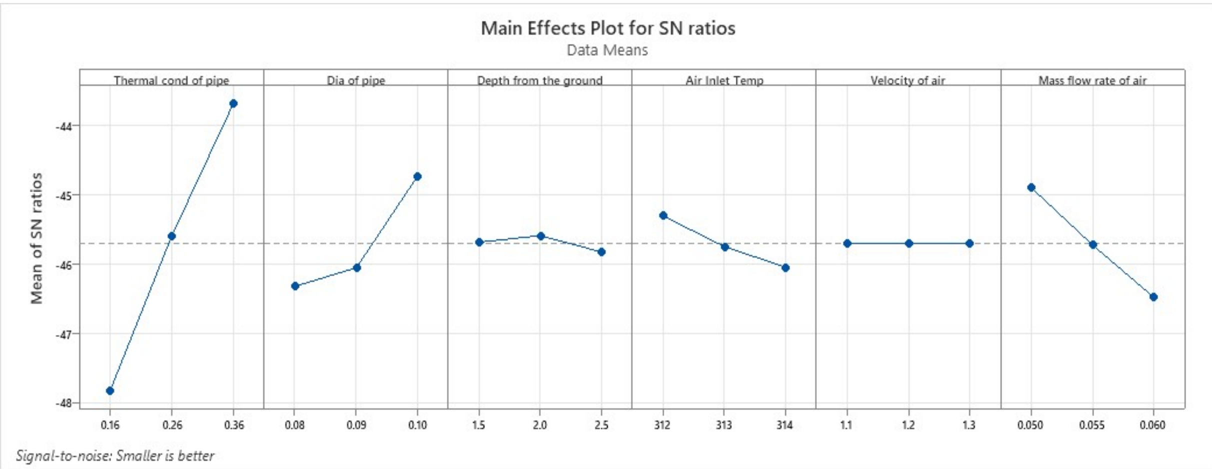

Figure no.3.2. S/N ratio graphs for Cooling condition

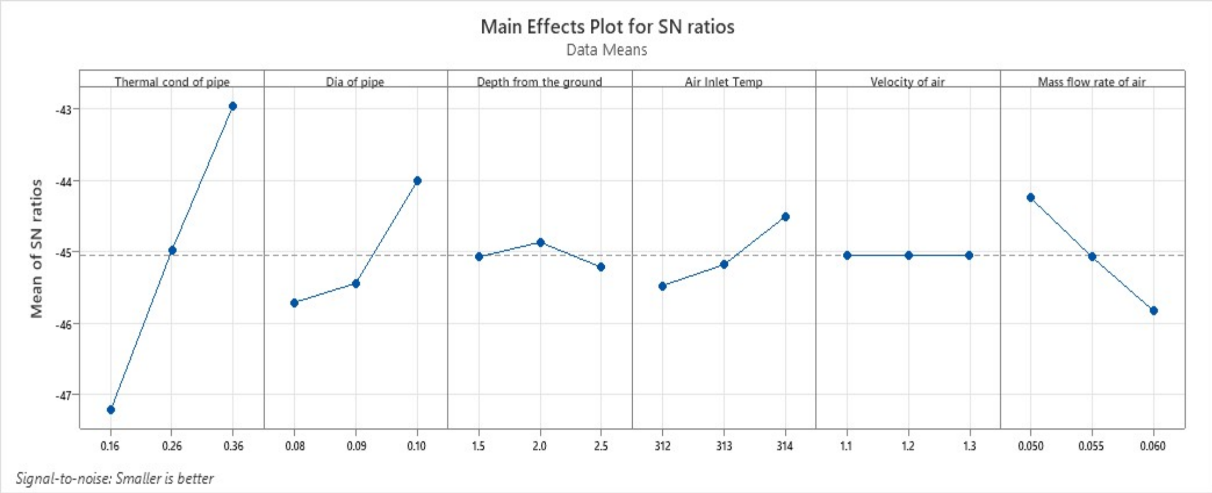

Figure no.3.3. S/N ratio graphs for Heating condition

And the values of optimum parameters are substituted in the Optimum space cooling and heating formula and the final value of the optimum length is obtained about 117 m for space cooling and 116 m for space heating.

3.8.2. S/N Ratio graphs for the Cooling load of 4.3 KW.

In the below table, K stands for Thermal conductivity of pipe (W/mK), D stands for Diameter of pipe (m), Dep stands for Depth from the ground (m), T_{in} stands for Air inlet Temperature (K), V_a stands for Velocity of air (m/s) and M_a stands for Mass flow rate of air (Kg/s).

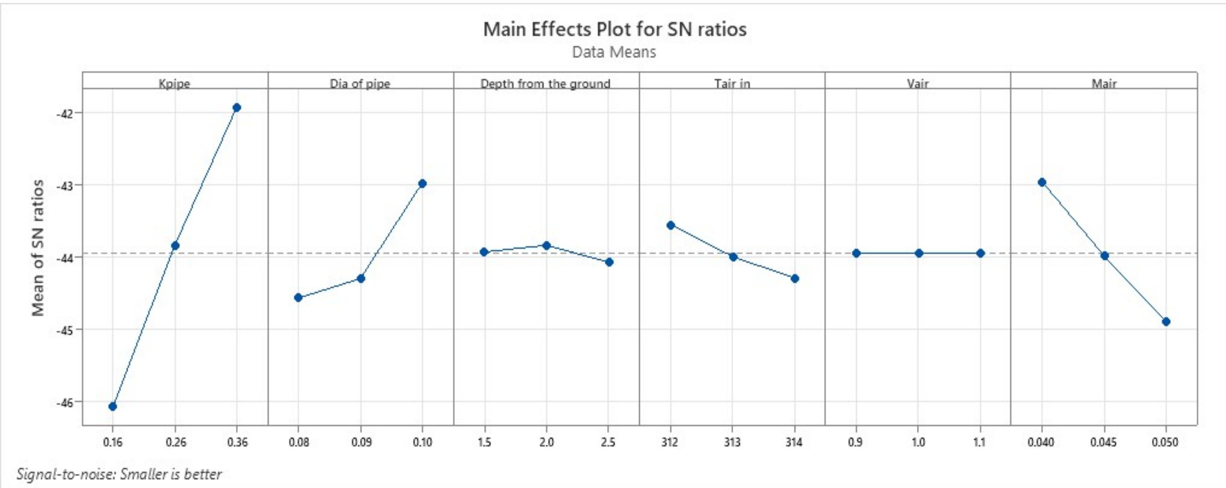

Figure no.3.4. S/N ratio graphs for Cooling condition

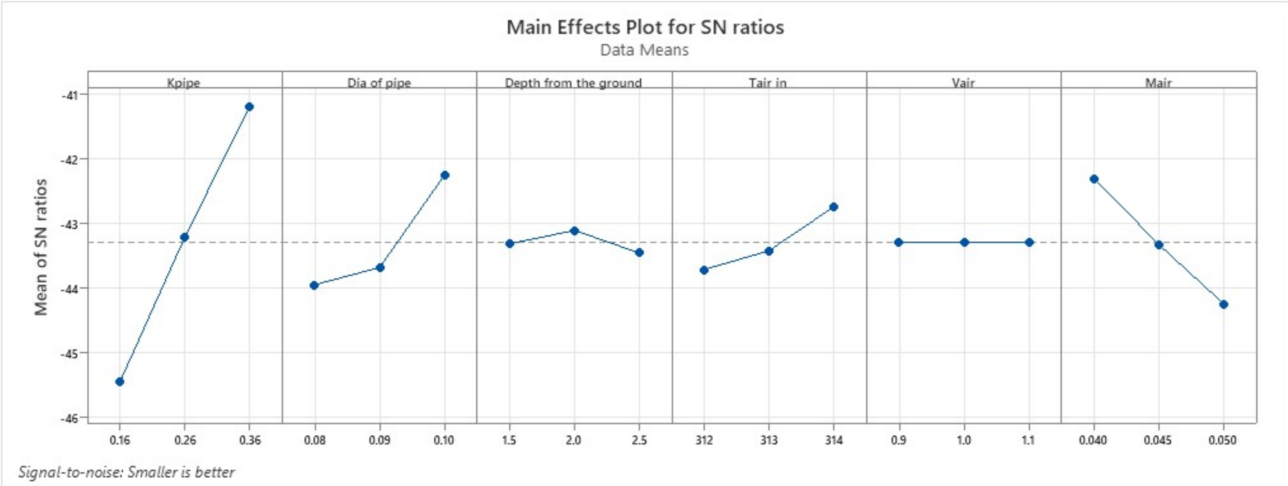

Figure no.3.5. S/N ratio graphs for Heating condition

And the values of optimum parameters are substituted in the Optimum space cooling and heating formula and the final value of the optimum length is obtained about 89 m for space cooling and 87 m for space heating.

3.8.3. S/N Ratio graphs for the Cooling load of 3.42 KW.

In the below table, K stands for Thermal conductivity of pipe (W/mK), D stands for Diameter of pipe (m), Dep stands for Depth from the ground (m), T_{in} stands for Air inlet Temperature (K), V_a stands for Velocity of air (m/s) and M_a stands for Mass flow rate of air (Kg/s).

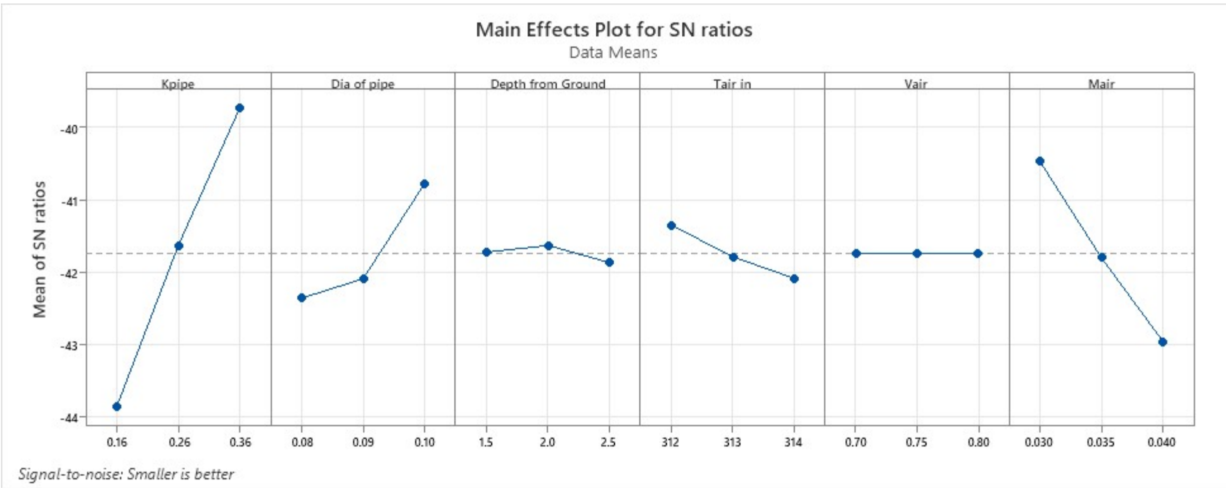

Figure no.3.6. S/N ratio graphs for Cooling condition

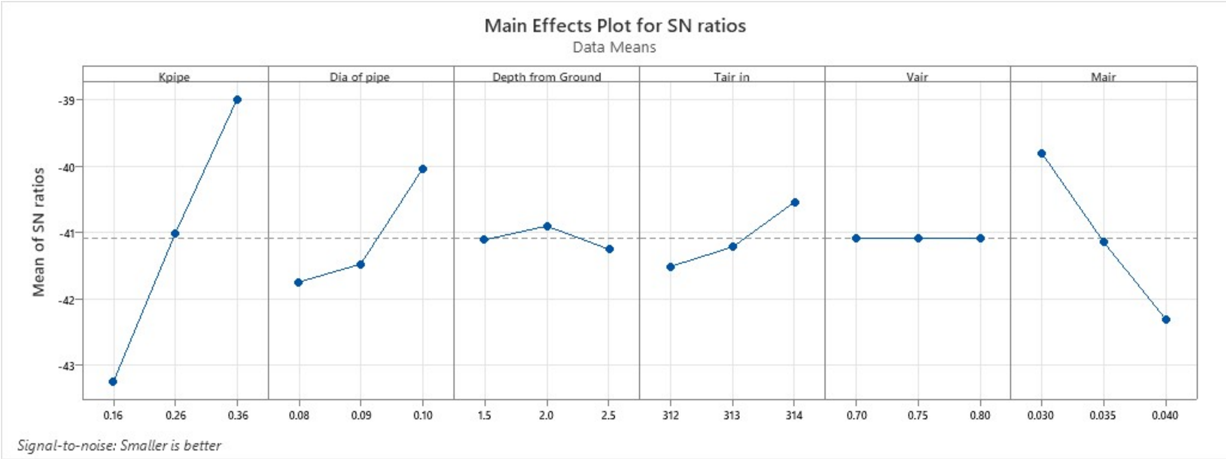

Figure no.3.7. S/N ratio graphs for Heating condition

And the values of optimum parameters are substituted in the Optimum space cooling and heating formula and the final value of the optimum length is obtained about 68 m for space cooling and 65 m for space heating.

3.8.4. S/N Ratio graphs for the Cooling load of 2.49 KW

In the below table, K stands for Thermal conductivity of pipe (W/mK), D stands for Diameter of pipe (m), Dep stands for Depth from the ground (m), T_{in} stands for Air inlet Temperature (K), V_a stands for Velocity of air (m/s) and M_a stands for Mass flow rate of air (Kg/s).

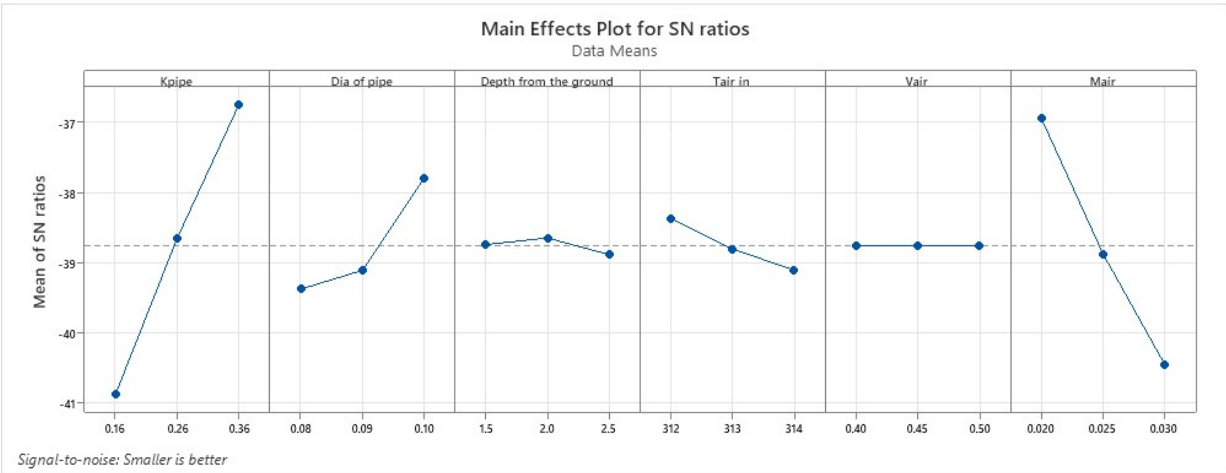

Figure no.3.8. S/N ratio graphs for Cooling condition

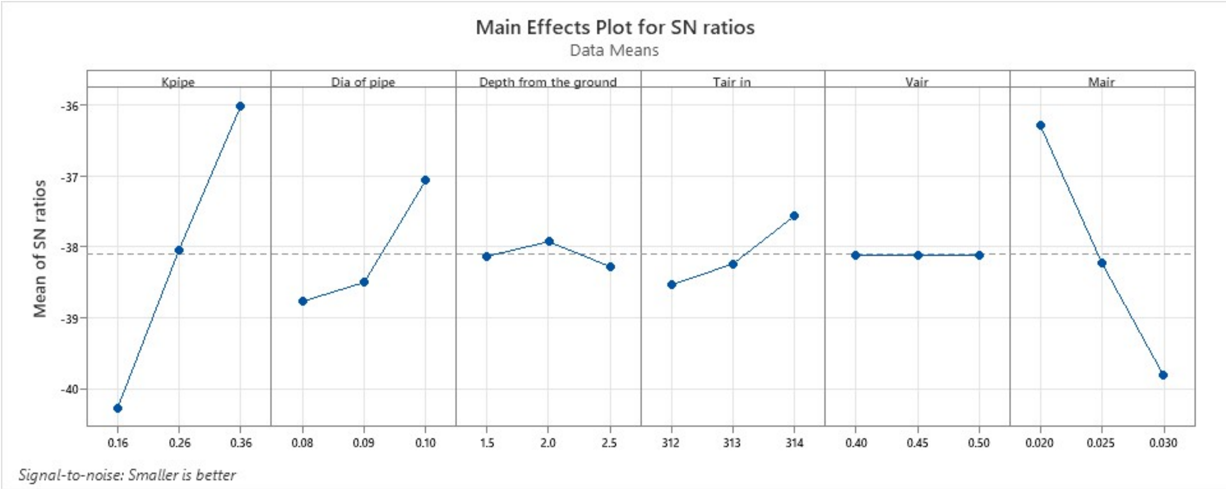

Figure no.3.9. S/N ratio graphs for Heating condition

And the values of optimum parameters are substituted in the Optimum space cooling and heating formula and the final value of the optimum length is obtained about 46 m for space cooling and 44.8 m for space heating.

3.8.5. S/N Ratio graphs for the Cooling load of 1.755 KW

In the below table, K stands for Thermal conductivity of pipe (W/mK), D stands for Diameter of pipe (m), Dep stands for Depth from the ground (m), T_{in} stands for Air inlet Temperature (K), V_a stands for Velocity of air (m/s) and M_a stands for Mass flow rate of air (Kg/s).

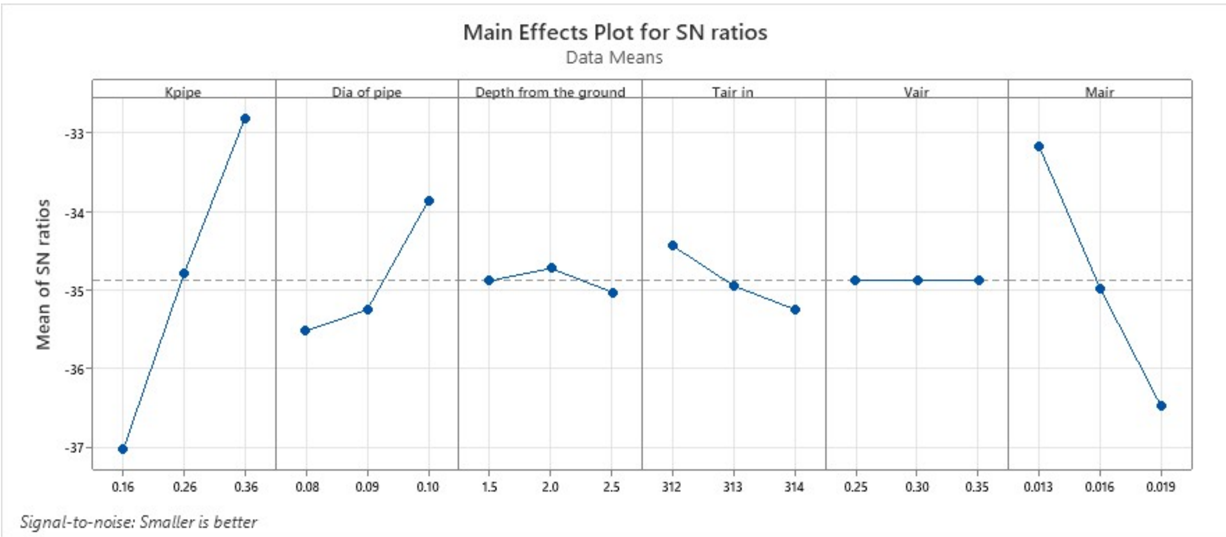

Figure no.3.10. S/N ratio graphs for Cooling condition

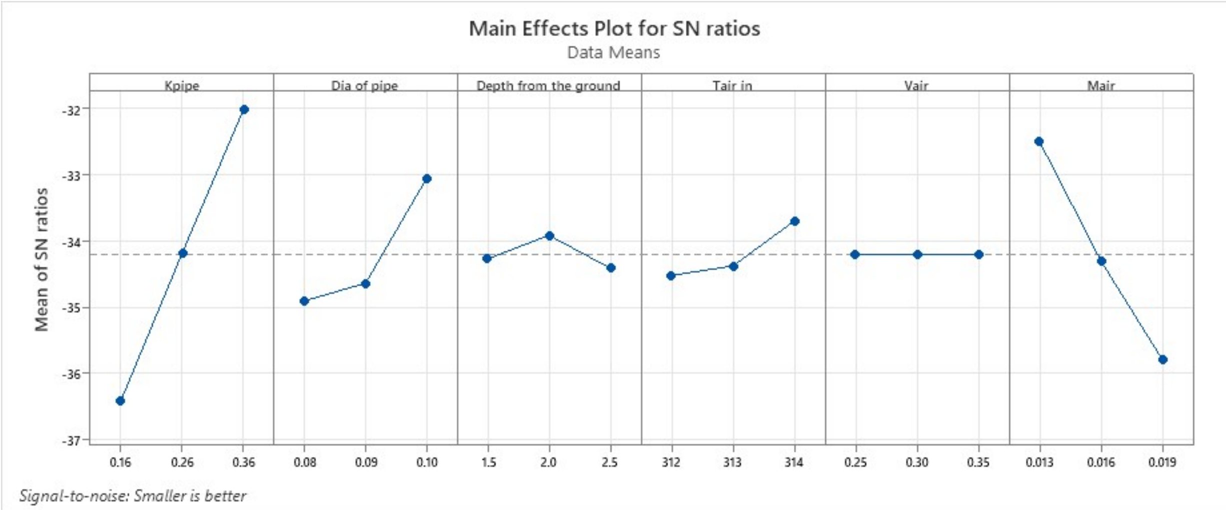

Figure no.3.11. S/N ratio graphs for Heating condition

And the values of optimum parameters are substituted in the Optimum space cooling and heating formula and the final value of the optimum length is obtained about 27.2 m for space cooling and 26 m for space heating.

3.8.6. S/N Ratio graphs for the Cooling load of 1.5 KW

In the below table, K stands for Thermal conductivity of pipe (W/mK), D stands for Diameter of pipe (m), Dep stands for Depth from the ground (m), T_{in} stands for Air inlet Temperature (K), V_a stands for Velocity of air (m/s) and M_a stands for Mass flow rate of air (Kg/s).

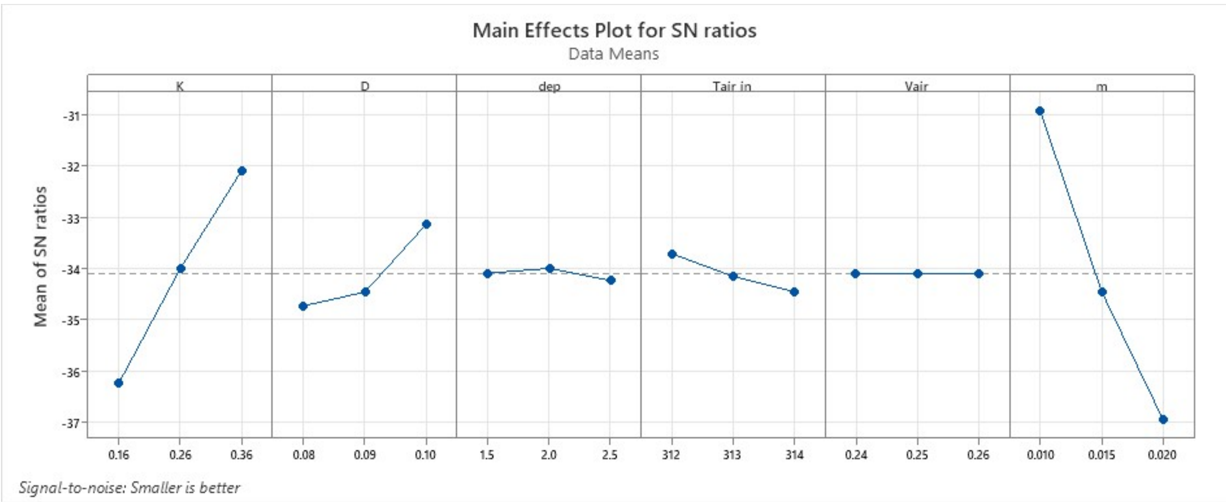

Figure no.3.12. S/N ratio graphs for Cooling condition

Fig.3.13. S/N ratio graphs for Heating condition

And the values of optimum parameters are substituted in the Optimum space cooling and heating formula and the final value of the optimum length is obtained about 23.5 m for space cooling and 23 m for space heating.

3.8.7. S/N Ratio graphs for the Cooling load of 0.44 KW

In the below table, K stands for Thermal conductivity of pipe (W/mK), D stands for Diameter of pipe (m), Dep stands for Depth from the ground (m), T_{in} stands for Air inlet Temperature (K), V_a stands for Velocity of air (m/s) and M_a stands for Mass flow rate of air (Kg/s).

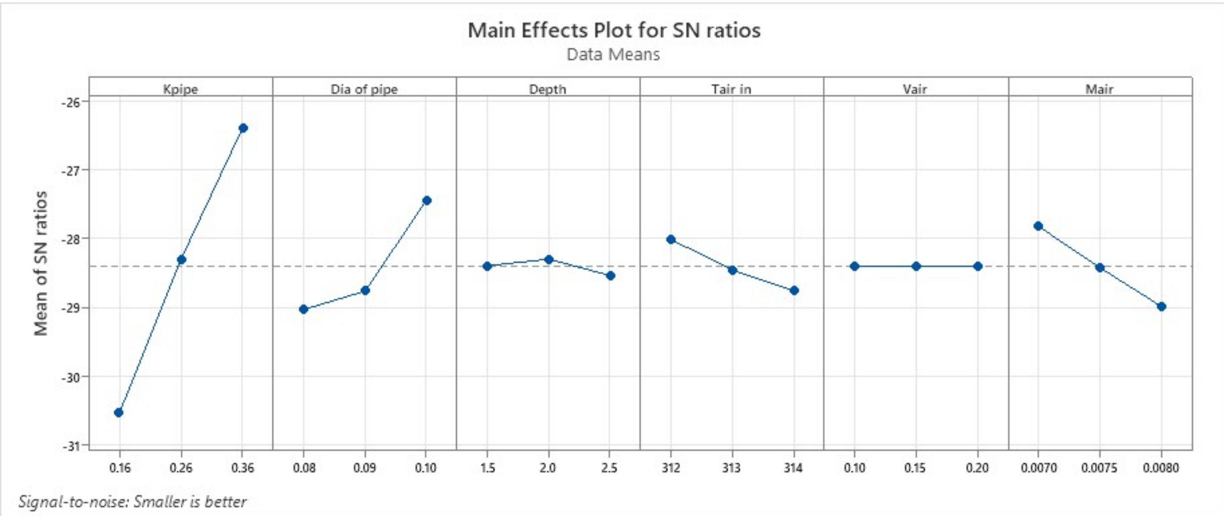

Figure no.3.14. S/N ratio graphs for Cooling condition

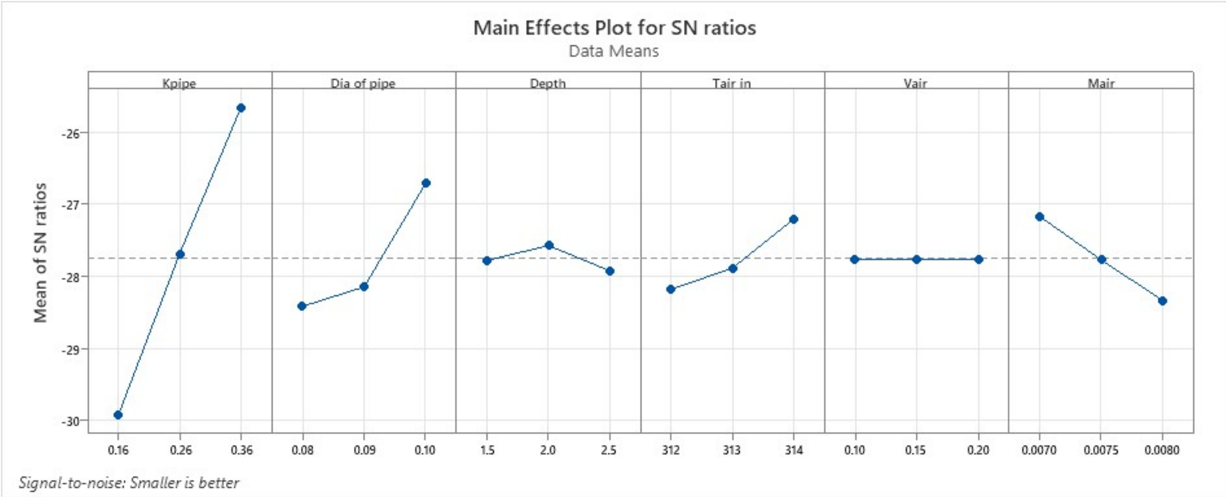

Figure no.3.15. S/N ratio graphs for Heating condition

And the values of optimum parameters are substituted in the Optimum space cooling and heating formula and the final value of the optimum length is obtained about 16.2 m for space cooling and 15.9 m for space heating.

3.8.8. S/N Ratio graphs for the Cooling load of 0.23 KW

In the below table, K stands for Thermal conductivity of pipe (W/mK), D stands for Diameter of pipe (m), Dep stands for Depth from the ground (m), T_{in} stands for Air inlet Temperature (K), V_a stands for Velocity of air (m/s) and M_a stands for Mass flow rate of air (Kg/s).

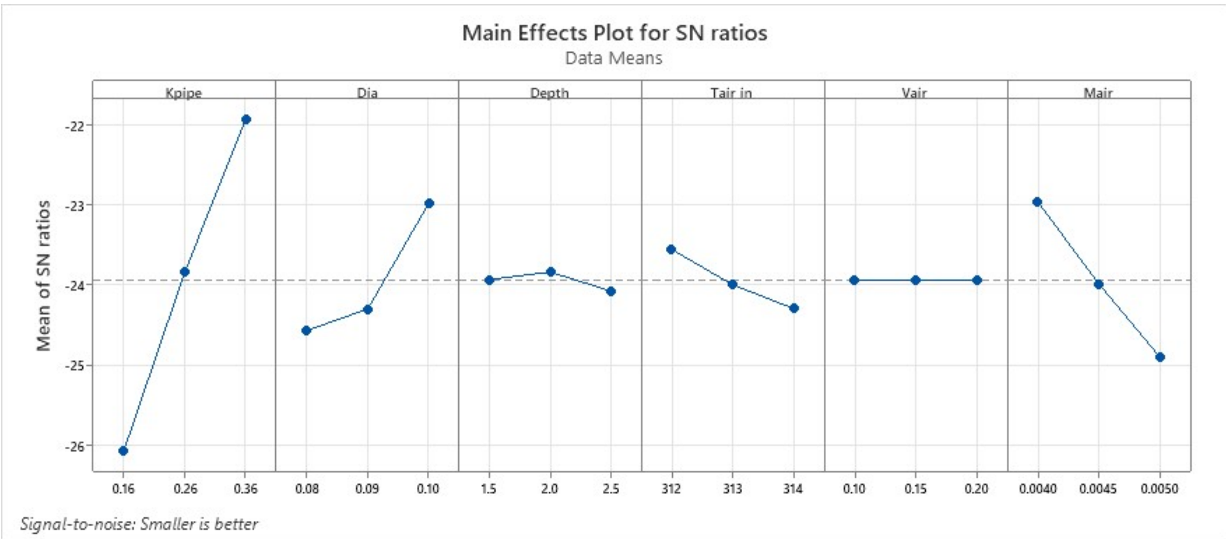

Figure no.3.16. S/N ratio graphs for Cooling condition

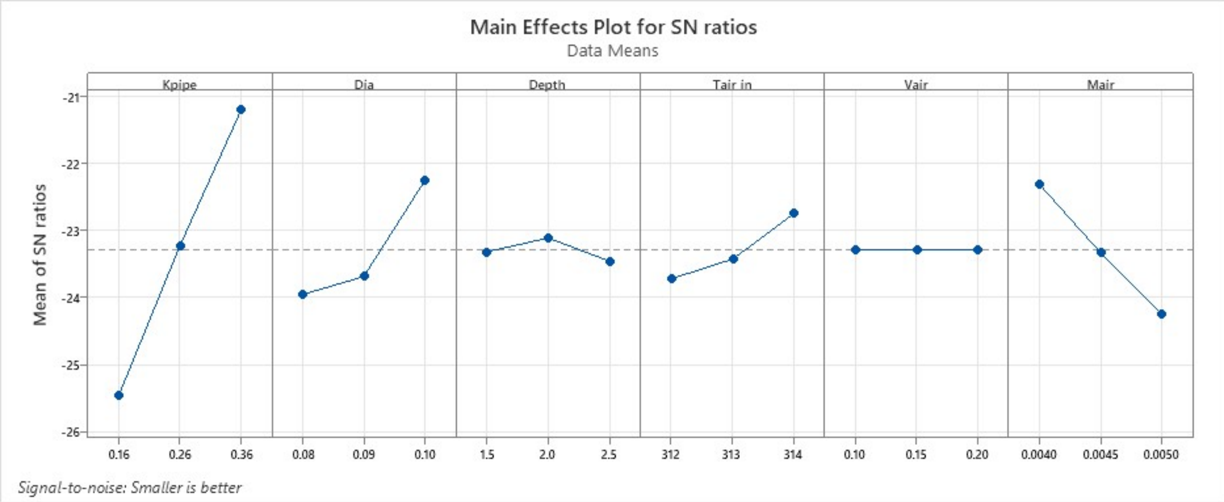

Figure no.3.17. S/N ratio graphs for Heating condition

And the values of optimum parameters are substituted in the Optimum space cooling and heating formula and the final value of the optimum length is obtained about 9.4 m for space cooling and 9 m for space heating.

3.8.9. S/N Ratio graphs for the Cooling load of 0.14 KW

In the below table, K stands for Thermal conductivity of pipe (W/mK), D stands for Diameter of pipe (m), Dep stands for Depth from the ground (m), T_{in} stands for Air inlet Temperature (K), V_a stands for Velocity of air (m/s) and M_a stands for Mass flow rate of air (Kg/s).

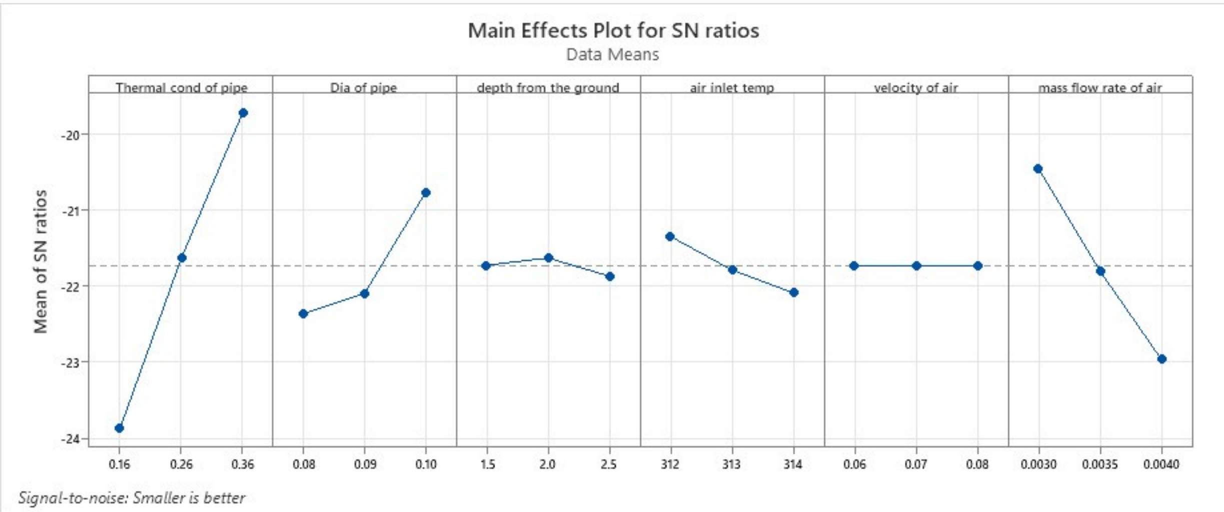

Figure no.3.18. S/N ratio graphs for Cooling condition

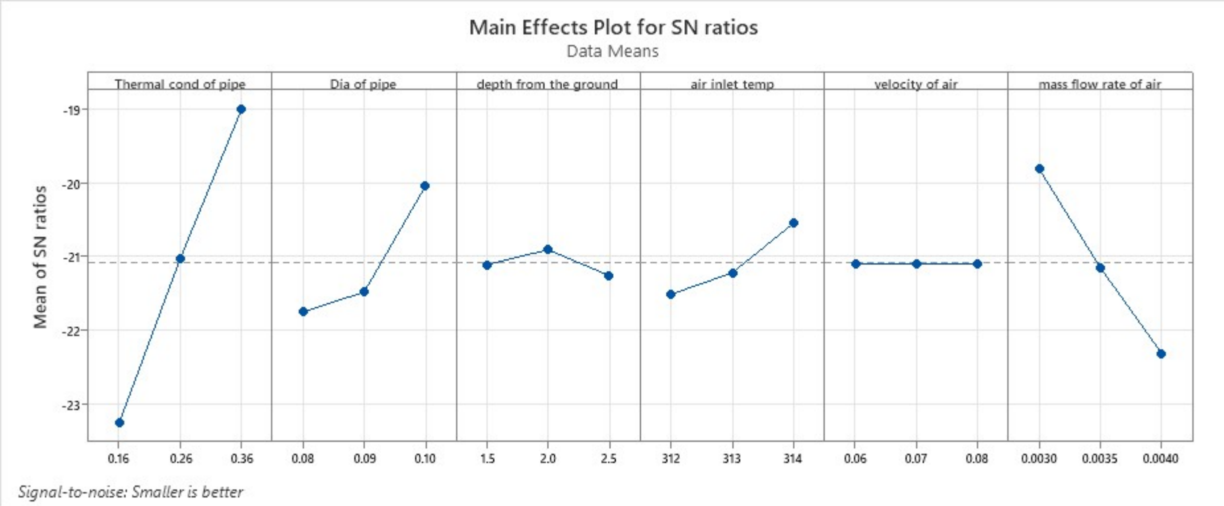

Figure no.3.19. S/N ratio graphs for Heating condition

And the values of optimum parameters are substituted in the Optimum space cooling and heating formula and the final value of the optimum length is obtained about 7 m for space cooling and 6.9 m for space heating.

3.9. Analysis of Variance (ANNOVA) Table:

Analysis of Variance generally indicates the percentage of contribution by each parameter impacting the performance of the system.

3.9.1. ANNOVA Table for 5.51 KW load

Table no 3.25. Analysis of Variance (ANNOVA) For space Cooling

Factors	Degree of freedom	Sum of squares (SS)	Variance	F-ratio	P-value	% Contribution
Thermal conductivity of pipe (W/mK)	2	39325	19662.4	38.97	0.00	76.46 %
Diameter of pipe (m)	2	5428	2714	1.42	0.262	10.55 %
Depth from the ground (m)	2	14.6	7.31	0.0	0.997	0.03 %
Air inlet Temperature (K)	2	599.4	299.7	0.14	0.869	1.17 %
Velocity of air (m/s)	2	108.3	54.17	0.03	0.975	0.21 %
Mass flow rate of air (Kg/s)	2	5817	2909	1.53	0.237	11.31 %
Error	14	142.7	71.35			0.277 %
Total	26	51435				100 %

Table no.3.26 Analysis of Variance (ANNOVA) For space Heating

Factors	Degree of freedom	Sum of squares (SS)	Variance	F-ratio	P-value	% Contribution
Thermal conductivity of pipe (W/mK)	2	37114	18557.2	28.54	0.00	70.40 %
Diameter of pipe (m)	2	7062	3531	1.86	0.178	13.40 %
Depth from the ground (m)	2	136.8	68.4	0.03	0.969	0.26 %
Air inlet Temperature (K)	2	3112	1556	0.75	0.482	5.90 %
Velocity of air (m/s)	2	102.2	51.12	0.02	0.977	0.19 %
Mass flow rate of air (Kg/s)	2	5031	2516	1.27	0.300	9.54 %
Error	14	160	80			0.3 %
Total	26	52718				100 %

3.9.2. ANNOVA Table for 4.3 KW load:

Table no 3.27. Analysis of Variance (ANNOVA) For space Cooling

Analysis of Variance

Source	DF	Seq SS	Contribution	Adj SS	Adj MS	F-Value	P-Value
Thermal conductivity of pipe (W/mK)	2	28481	83.30%	28481	14240.4	59.84	0.000
Diameter of pipe (m)	2	1096	3.21%	1096	548.2	0.40	0.676
Depth from the ground(m)	2	47.9	0.14%	47.9	23.93	0.02	0.983
Air inlet Temperature (K)	2	362.9	1.06%	362.9	181.5	0.13	0.880
Velocity of air (m/s)	2	117.2	0.34%	117.2	58.60	0.04	0.960
Mass flow rate of air (Kg/s)	2	3957	11.57%	3957	1979	1.57	0.229
Error	14	130	0.38%	130	65		
Total	26	34192	100.00%				

Table no 3.28. Analysis of Variance (ANNOVA) For space Heating

Analysis of Variance

Source	DF	Seq SS	Contribution	Adj SS	Adj MS	F-Value	P-Value
Thermal conductivity of pipe (W/mK)	2	25400	78.75%	25400	12700.2	44.47	0.000
Diameter of pipe (m)	2	1601	4.97%	1601	800.7	0.63	0.543
Depth from the ground(m)	2	50.7	0.16%	50.7	25.36	0.02	0.981

Air inlet Temperature (K)	2	1525	4.73%	1525	762.3	0.60	0.559
Velocity of air (m/s)	2	104.5	0.32%	104.5	52.26	0.04	0.962
Mass flow rate of air (Kg/s)	2	3442	10.67%	3442	1721	1.43	0.258
Error	14	131.8	0.41%	131.8	65.9		
Total	26	32255	100.00%				

3.9.3. ANNOVA Table for 3.42 KW load:

Table no 3.29. Analysis of Variance (ANNOVA) For space Cooling

Analysis of Variance

Source	DF	Seq SS	Contribution	Adj SS	Adj MS	F-Value	P-Value
Thermal conductivity of pipe (W/mK)	2	17229	77.10%	17229	8614.5	40.41	0.000
Diameter of pipe (m)	2	663.3	2.97%	663.3	331.6	0.37	0.697
Depth from the ground (m)	2	29.0	0.13%	29.0	14.48	0.02	0.985
Air inlet Temperature (K)	2	219.5	0.98%	219.5	109.8	0.12	0.888
Velocity of air (m/s)	2	117.2	0.52%	117.2	58.60	0.06	0.939
Mass flow rate of air (Kg/s)	2	3957	17.71%	3957	1978.7	2.58	0.096
Error	14	130	0.58%	130	65		
Total	26	22345.0	100.00%				

Table no 3.30. Analysis of Variance (ANNOVA) For space Heating

Analysis of Variance

Source	DF	Seq SS	Contribution	Adj SS	Adj MS	F-Value	P-Value
Thermal conductivity of pipe (W/mK)	2	15366	73.29%	15366	7682.8	32.93	0.000
Diameter of pipe (m)	2	968.8	4.62%	968.8	484.4	0.58	0.567
Depth from the ground(m)	2	30.7	0.15%	30.7	15.34	0.02	0.983
Air inlet Temperature (K)	2	922.2	4.40%	922.2	461.1	0.55	0.583
Velocity of air (m/s)	2	104.5	0.50%	104.5	52.26	0.06	0.942
Mass flow rate of air (Kg/s)	2	3442	16.42%	3442	1721.2	2.36	0.116
Error	14	130.7	0.623%	130.7	65.35		
Total	26	20964.9	100.00%				

3.9.4. ANNOVA Table for 2.49 KW load:

Table no 3.31. Analysis of Variance (ANNOVA) For space Cooling

Analysis of Variance

Source	DF	Seq SS	Contribution	Adj SS	Adj MS	F-Value	P-Value
Thermal conductivity of pipe (W/mK)	2	8790	65.31%	8790	4395.2	22.59	0.000
Diameter of pipe (m)	2	338.4	2.51%	338.4	169.2	0.31	0.737
Depth from the ground(m)	2	14.8	0.11%	14.8	7.387	0.01	0.987
Air inlet Temperature (K)	2	112.0	0.83%	112.0	56.01	0.10	0.905
Velocity of air (m/s)	2	117.2	0.87%	117.2	58.60	0.11	0.900
Mass flow rate of air (Kg/s)	2	3957	29.40%	3957	1978.7	5.00	0.015
Error	14	130.3	0.97%	130.3	65.15		
Total	26	13459.7	100.00%				

Table no 3.32. Analysis of Variance (ANNOVA) For space Heating

Analysis of Variance

Source	DF	Seq SS	Contribution	Adj SS	Adj MS	F-Value	P-Value
Thermal conductivity of pipe (W/mK)	2	7840	62.73%	7840	3919.8	20.20	0.000
Diameter of pipe (m)	2	494.3	3.96%	494.3	247.1	0.49	0.616
Depth from the ground (m)	2	15.7	0.13%	15.7	7.828	0.02	0.985
Air inlet Temperature (K)	2	470.5	3.76%	470.5	235.3	0.47	0.631
Velocity of air (m/s)	2	104.5	0.84%	104.5	52.26	0.10	0.904
Mass flow rate of air (Kg/s)	2	3442	27.54%	3442	1721.2	4.56	0.021
Error	14	131	1.048%	131	65.5		
Total	26	12498	100.00%				

3.9.5. ANNOVA Table for 1.755 KW load:

Table no 3.33. Analysis of Variance (ANNOVA) For space Cooling

Analysis of Variance

Source	DF	Seq SS	Contribution	Adj SS	Adj MS	F-Value	P-Value
Thermal conductivity of pipe (W/mK)	2	17229	77.10%	17229	8614.5	40.41	0.000
Diameter of pipe (m)	2	663.3	2.97%	663.3	331.6	0.37	0.697
Depth from the ground(m)	2	29.0	0.13%	29.0	14.48	0.02	0.985
Air inlet Temperature (K)	2	219.5	0.98%	219.5	109.8	0.12	0.888
Velocity of air (m/s)	2	117.2	0.52%	117.2	58.60	0.06	0.939
Mass flow rate of air	2	3957	17.71%	3957	1978.7	2.58	0.096

(Kg/s)							
Error	14	130	0.58%	130	65		
Total	26	22345.0	100.00%				

Table no 3.34. Analysis of Variance (ANNOVA) For space Heating

Analysis of Variance

Source	DF	Seq SS	Contribution	Adj SS	Adj MS	F-Value	P-Value
Thermal conductivity of pipe (W/mK)	2	15366	73.29%	15366	7682.8	32.93	0.000
Diameter of pipe (m)	2	968.8	4.62%	968.8	484.4	0.58	0.567
Depth from the ground(m)	2	30.7	0.15%	30.7	15.34	0.02	0.983
Air inlet Temperature (K)	2	922.2	4.40%	922.2	461.1	0.55	0.583
Velocity of air (m/s)	2	104.5	0.50%	104.5	52.26	0.06	0.942
Mass flow rate of air (Kg/s)	2	3442	16.42%	3442	1721.2	2.36	0.116
Error	14	130.7	0.623%	130.7	65.35		
Total	26	20964.9	100.00%				

3.9.6. ANNOVA Table for 1.5 KW load:

Table no 3.35. Analysis of Variance (ANNOVA) For space Cooling

Analysis of Variance

Source	DF	Seq SS	Contribution	Adj SS	Adj MS	F-Value	P-Value
Thermal conductivity of pipe (W/mK)	2	3195	42.48%	3195	1597.4	8.86	0.001
Diameter of pipe (m)	2	123.8	1.65%	123.8	61.90	0.20	0.819
Depth from the ground(m)	2	4.44	0.06%	4.44	2.220	0.01	0.993
Air inlet Temperature (K)	2	41.27	0.55%	41.27	20.63	0.07	0.936
Velocity of air (m/s)	2	113.6	1.51%	113.6	56.81	0.18	0.833
Mass flow rate of air (Kg/s)	2	3907	51.96%	3907	1953.5	12.98	0.000
Error	14	134.89	1.8%	134.89	67.45		
Total	26	7520	100.00%				

Table no 3.36. Analysis of Variance (ANNOVA) For space Heating

Analysis of Variance

Source	DF	Seq SS	Contribution	Adj SS	Adj MS	F-Value	P-Value
Thermal conductivity of	2	2872	41.82%	2872	1436.1	8.63	0.002

pipe (W/mK)							
Diameter of pipe (m)	2	195.0	2.84%	195.0	97.50	0.35	0.708
Depth from the ground(m)	2	2.53	0.04%	2.53	1.267	0.00	0.996
Air inlet Temperature (K)	2	159.6	2.32%	159.6	79.81	0.29	0.754
Velocity of air (m/s)	2	96.39	1.40%	96.39	48.20	0.17	0.844
Mass flow rate of air (Kg/s)	2	3420	49.79%	3420	1709.9	11.90	0.000
Error	14	122.48	1.78%	122.48	61.24		
Total	26	6868	100.00%				

3.9.7. ANNOVA Table for 0.4 KW load:

Table no 3.37. Analysis of Variance (ANNOVA) For space Cooling

Analysis of Variance

Source	DF	Seq SS	Contribution	Adj SS	Adj MS	F-Value	P-Value
Thermal conductivity of pipe (W/mK)	2	900.1	80.66%	900.1	450.066	50.05	0.000
Diameter of pipe (m)	2	34.65	3.11%	34.65	17.33	0.38	0.685
Depth from the ground (m)	2	1.51	0.14%	1.51	0.7564	0.02	0.984
Air inlet Temperature (K)	2	11.47	1.03%	11.47	5.735	0.12	0.883
Velocity of air (m/s)	2	4.69	0.42%	4.69	2.344	0.05	0.951
Mass flow rate of air (Kg/s)	2	158.3	14.18%	158.3	79.15	1.98	0.160
Error	14	5.21	0.4668%	5.21	2.65		
Total	26	1115.93	100.00%				

Table no 3.38. Analysis of Variance (ANNOVA) For space Heating

Analysis of Variance

Source	DF	Seq SS	Contribution	Adj SS	Adj MS	F-Value	P-Value
Thermal conductivity of pipe (W/mK)	2	802.8	76.43%	802.8	401.39	38.92	0.000
Diameter of pipe (m)	2	50.62	4.82%	50.62	25.31	0.61	0.553
Depth from the ground (m)	2	1.60	0.15%	1.60	0.8016	0.02	0.982
Air inlet Temperature (K)	2	48.18	4.59%	48.18	24.09	0.58	0.569
Velocity of air (m/s)	2	4.18	0.40%	4.18	2.091	0.05	0.953
Mass flow rate of air (Kg/s)	2	137.7	13.11%	137.7	68.85	1.81	0.185
Error	14	5.22	0.4668%	5.22	2.66		
Total	26	1050.3	100.00%				

3.9.8. ANNOVA Table for 0.23 KW load:

Table no 3.39. Analysis of Variance (ANNOVA) For space Cooling

Analysis of Variance

Source	DF	Seq SS	Contribution	Adj SS	Adj MS	F-Value	P-Value
Thermal conductivity of pipe (W/mK)	2	284.81	83.30%	284.81	142.404	59.84	0.000
Diameter of pipe (m)	2	10.96	3.21%	10.96	5.482	0.40	0.676
Depth from the ground (m)	2	0.479	0.14%	0.479	0.2393	0.02	0.983
Air inlet Temperature (K)	2	3.629	1.06%	3.629	1.815	0.13	0.880
Mass flow rate of air (Kg/s)	2	39.57	11.57%	39.57	19.79	1.57	0.229
Error	16	2.472	0.73%	2.472	1.236		
Total	26	341.92	100.00%				

Table no 3.40. Analysis of Variance (ANNOVA) For space Heating

Analysis of Variance

Source	DF	Seq SS	Contribution	Adj SS	Adj MS	F-Value	P-Value
Thermal conductivity of pipe (W/mK)	2	254.00	78.75%	254.00	127.002	44.47	0.000
Diameter of pipe (m)	2	16.01	4.97%	16.01	8.007	0.63	0.543
Depth from the ground (m)	2	0.507	0.16%	0.507	0.2536	0.02	0.981
Air inlet Temperature (K)	2	15.25	4.73%	15.25	7.623	0.60	0.559
Mass flow rate of air (Kg/s)	2	34.42	10.67%	34.42	17.21	1.43	0.258
Error	16	2.36	0.73%	2.36	1.18		
Total	26	322.55	100.00%				

3.9.9. ANNOVA Table for 0.14 KW load:

Table no 3.41. Analysis of Variance (ANNOVA) For space Cooling

Analysis of Variance

Source	DF	Seq SS	Contribution	Adj SS	Adj MS	F-Value	P-Value
Thermal conductivity of pipe (W/mK)	2	172.29	77.10%	172.29	86.145	40.41	0.000

Diameter of pipe (m)	2	6.633	2.97%	6.633	3.316	0.37	0.697
Depth from the ground (m)	2	0.290	0.13%	0.290	0.1448	0.02	0.985
Air inlet Temperature (K)	2	2.195	0.98%	2.195	1.098	0.12	0.888
Mass flow rate of air (Kg/s)	2	39.57	17.71%	39.57	19.787	2.58	0.096
Error	16	2.36	0.73%	2.36	1.18		
Total	26	223.450	100.00%				

Table no 3.42. Analysis of Variance (ANNOVA) For space Heating

Analysis of Variance

Source	DF	Seq SS	Contribution	Adj SS	Adj MS	F-Value	P-Value
Thermal conductivity of pipe (W/mK)	2	153.66	73.29%	153.66	76.828	32.93	0.000
Diameter of pipe (m)	2	9.688	4.62%	9.688	4.844	0.58	0.567
Depth from the ground (m)	2	0.307	0.15%	0.307	0.1534	0.02	0.983
Air inlet Temperature (K)	2	9.222	4.40%	9.222	4.611	0.55	0.583
Mass flow rate of air (Kg/s)	2	34.42	16.42%	34.42	17.212	2.36	0.116
Error	16	2.36	1.12%	2.36	1.18		
Total	26	209.649	100.00%				

From the above ANNOVA Tables, it was clearly observed that the Thermal conductivity of the pipe material, Diameter of the pipe, Inlet air temperature and the mass flow rate of the air are the major contributors in order to improve the performance of the geothermal air conditioner.

3.10. Governing equations for Simulation:

In the geothermal air conditioner, fluid flow phenomenon is governed by the continuity, momentum and energy equations. The equations are as follows:

Continuity equation:

$$\frac{\partial \rho}{\partial t} + \nabla.(\rho\vec{u}) = 0 \tag{19}$$

Momentum equation:

$$\frac{\partial(\rho\vec{u})}{\partial t} + \nabla.(\rho\vec{u}\vec{u}) = \rho\vec{g} - \nabla p + \nabla.(\bar{\bar{\tau}}) + \vec{F} \tag{20}$$

Energy equation:

$$\frac{\partial(\rho E)}{\partial t} + \nabla.(\vec{u}\ (\rho\ E + p)) = \nabla\ .\ (k_{\text{eff}}\nabla T + (\tau_{\text{eff}}.\vec{u})) \qquad (21)$$

Where, p is the static pressure, $\bar{\bar{\tau}}$ is the stress tensor and $\rho\vec{g}$ and $\vec{F}$ are the gravitational body force and external body forces, respectively

In the present study, above governing equations are solved by the finite volume method with the help of ANSYS FLUENT 19.2.

The following assumptions were used to solve this problem:

- The heat transfer and fluid flow involves single phase, incompressible and steady state.
- Fully developed turbulent flow was considered.
- The heat transfer takes place by convection, conduction and from soil.
- No radiation heat transfer.

Chapter 4

Design and Project Execution

4.1. Proposed Experimental Setup:

In this Project, Design of Experiment was carried out by using Taguchi method in order to achieve the optimum parameters of the geothermal air conditioning test rig for reducing the cooling as well as the heating load. For the study six parameters at three different levels were considered. And the analysis of variance method (ANNOVA) is used to identify the contribution of each parameter on the performance of the geothermal heat exchanger. The design part comprises of pipe arrangement in series and inner and outer chamber that was developed during the project. The pipe arrangement as well as box was Designed using Autodesk Fusion 360 software. And the analysis of the pipe arrangement was carried out using ANSYS FLUENT software. The inner and outer boxes of the test rig are fabricated and one end of both chamber fixed with nut and bolt in order to open and close the chamber. The inner chamber comprises of soil and pipe arrangement. The air conditioning test rig is used for maintaining the required temperature of soil inside the chamber. Further the air from the outlet of the air conditioning test rig is supplied to the cold storage in order to reduce the work done by the compressor. The experimental setup of the proposed geothermal air conditioning test rig is shown in the below figure no.4.1.

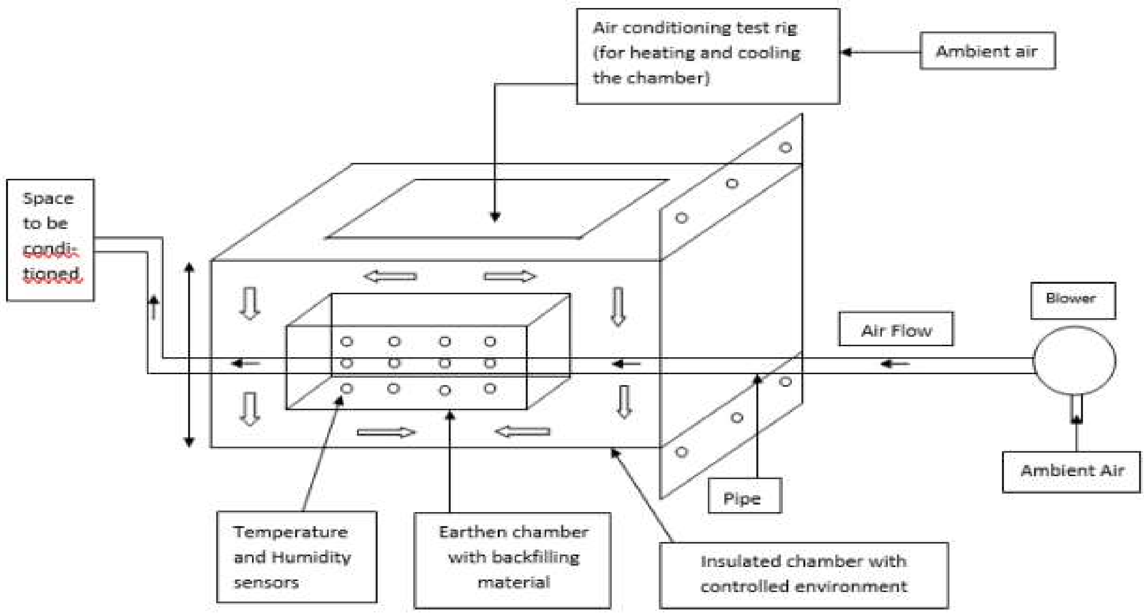

Fig. 4.1.Experimental setup diagram of Proposed Geothermal Air Conditioning Test Rig

The above (fig 1.2) shows the experimental setup of the geothermal air conditioning test rig. The blower supplies the air through pipe which is passed through the earthen chamber. The earthen chamber is filled with the backfilling material and air conditioning test rig is connected to the above chamber in order to maintain the required temperature of the backfilling material. Then the conditioned air is supplied to space which is to be conditioned. The temperature and humidity sensors will be present in the earthen chamber in order to check the temperature and humidity of the backfilling material. The above project is funded by ISHRAE and Pimpri chinchwad college of Engineering. ISHRAE has provided the funding of Rs. 100000/- and PCCOE has given the funding of Rs. 50000/-.

4.2. Design of Inner and Outer chamber:

The outer and inner chambers were first designed using AUTODESK Fusion 360 software. The outer chamber was made fully insulated and having dimensions of 1.5m*1.5m*1.5m whereas as the inner chamber was made using perforated sheets in order to enhance the heat transfer rate in the soil and having dimensions of 1.4m*1.4m*1.25m. The design of outer chamber and the inner chamber are shown in the below figure no 4.2. and figure no 4.3.

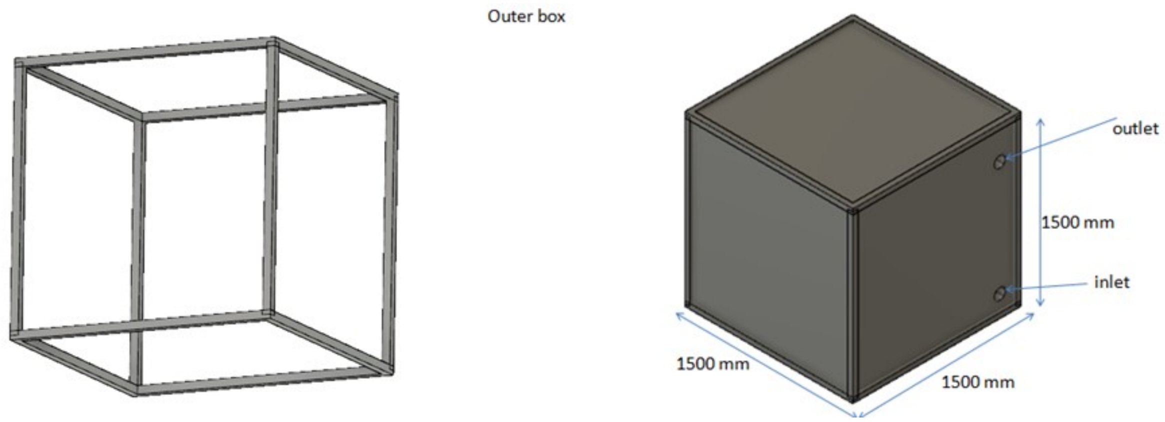

Figure no. 4. 2. Design of outer chamber

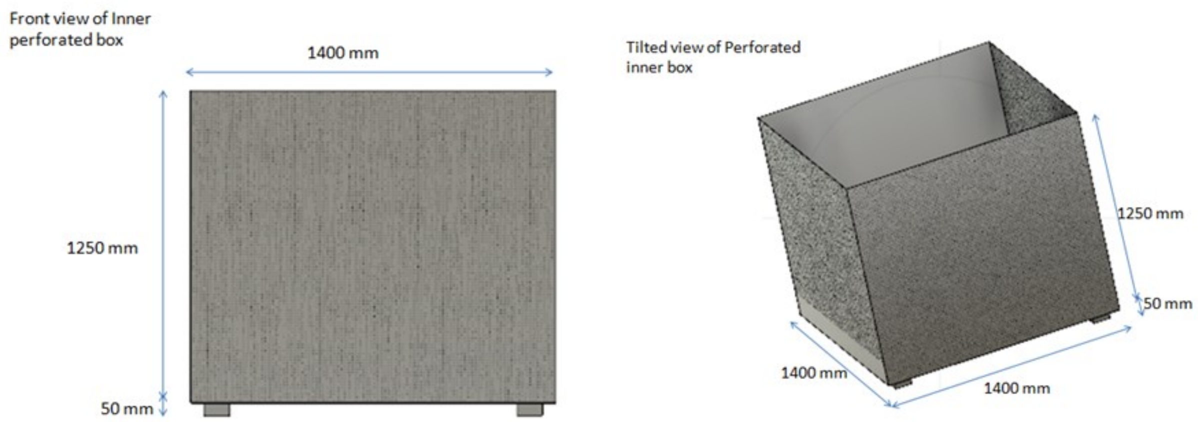

Figure no 4. 3. Design of Inner perforated chamber

4.3. Design of Pipe Arrangement:

4.3.1. Geometry of the pipe:

The pipe arrangement that is used in the project was made up of PVC and the arrangement comprises of 5 pipes in one layer and having four such layers. Length of each pipe was 1.2 m and the distance between the two pipes was maintained with 0.2 m gap. The design of this pipe arrangement was made using AUTODESK Fusion 360 software. These pipes were later fitted in the inner perforated chamber along with the soil. The design of actual pipe arrangement with its dimensions are shown in the below figure no 4.4. And the four views of the pipe arrangement are shown by the below figure 4.5.

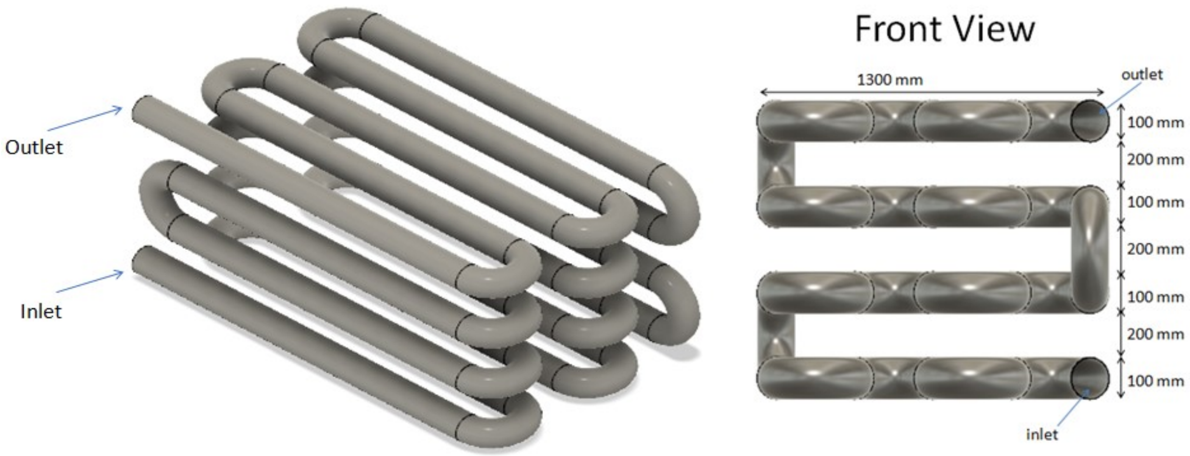

Figure no 4. 4. Design of the actual pipe arrangement

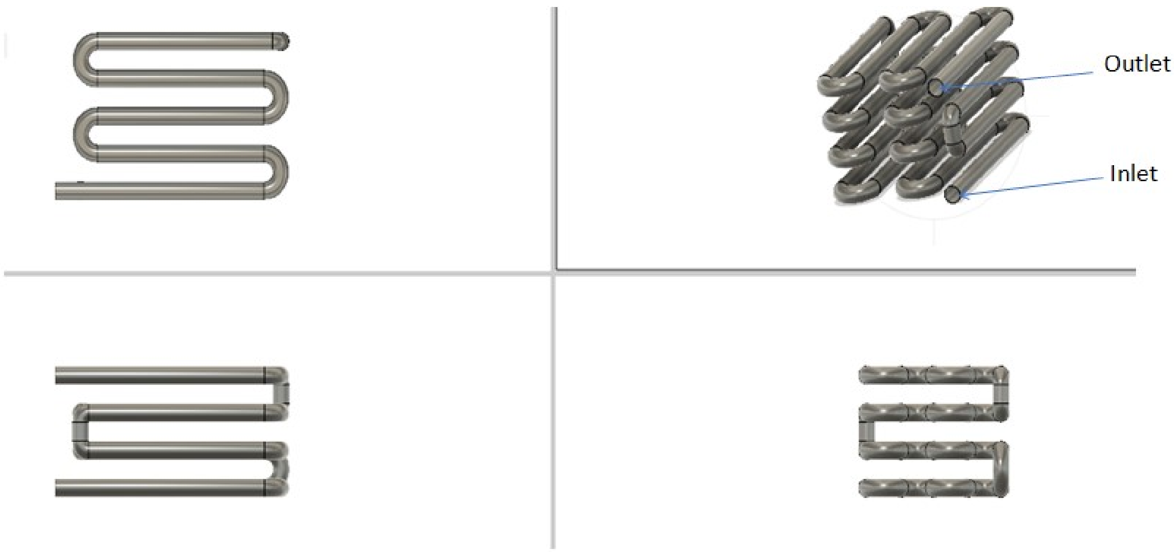

Figure no 4. 5. Four views of the pipe arrangement

4.3.2. Meshing:

The geometry of the pipe arrangement was imported in the ANSYS Fluent software for meshing and further analysis. For meshing of the pipe geometry POLYHEDRA MESH was used with maximum and minimum size of 0.0001m to 0.008m. After meshing the orthogonal quality of the mesh was found to be 0.83, while skewness was about 0.2. The number of nodes was equal to 2087922 and the number of elements was 1796332.The below figure 4.6. shows the meshing of the pipe arrangement.

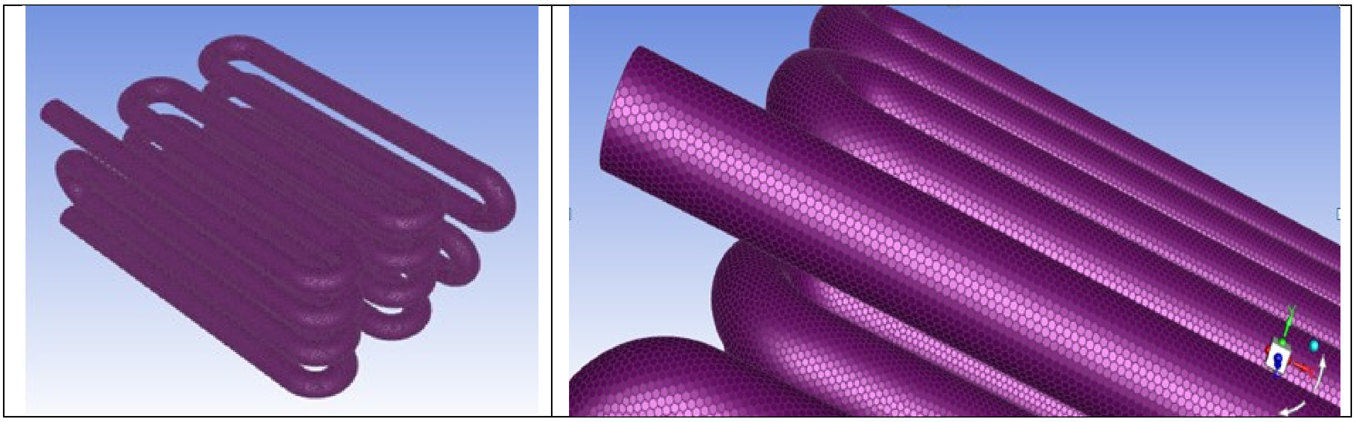

Figure no 4. 6. Meshing of the pipe

4.3.3. Boundary Conditions:

For the CFD analysis few boundary conditions were considered. The boundary conditions are:

1) Air Inlet temperature- 312 K
2) Air inlet velocity- 1.12 m/s
3) Convective Heat transfer coefficient- 29.11 W/m^2K
4) Temperature of the pipe surface- 297K.
5) Material of the Pipe- PVC.
6) Energy Equation- ON
7) K-Epsilon Turbulence model with standard wall realizable function.

4.4. Core Cutter test:

In order to measure the moisture content present in the soil and identify the density of the soil of Pune location, Core Cutter test method was used. The figure 4.7. shows the equipments required for performing the core cutter test.

Figure no 4. 7. Equipments used in Core cutter test

In the core cutter test, the core cutter with dolly is inserted in the soil. Dolly is generally provided for the factor of safety. After inserting the entire core cutter in the soil, the chisel and pellet knife was used to remove the soil from the surrounding core cutter. The soil sample collected in the core cutter is shown in the figure 4.8.

Figure no 4. 8. Soil sample collected in the core cutter

Then the initial mass of the container (S1/46) and (S1/2) was measured with the help of weighing machine as shown in the figure 4.9.

Mass M1 (S1/46) = 13.1 gram

Mass M1 (S1/2) = 13 gram

Now Weight of the container after filling the soil is shown by the figure 4.10.

Mass M2 (S1/46) = 114 gram

Mass M2 (S1/2) = 105 gram

Figure no 4. 9. Weighting of the empty container.

Figure no 4. 10. Containers filled with soil

The containers filled with the soil were kept in the oven at 105 degree Celsius for 24 hours. The mass of the container after 24 hours is shown below in the figure no 4.11:

Mass m3 (S1/46) = 105.6 gram

Mass m3 (S1/2) = 100.8 gram

Figure no 4.11. Weight of the container after 24 Hours

Now in order to identify the moisture content present in soil following formula was used. [20]

$\omega = [(M2 - M3)/(M3 - M1)] \times 100$

Where,

ω = Percentage of moisture content present in the soil

M1 = Mass of the empty container

M2 = Mass of the container with soil

M3 = Mass of soil without water content

So by substituting the values of masses in the above given formula,

We get

ω for (S1/46) = 9.08 %

ω for (S1/2) = 4.78 %

Therefore, the moisture content present in the soil can be measured by taking the average of both the values i.e.

ω = 6.93 %

Now the weight of the core cutter without filling the soil =896 gram

The weight of the core cutter after filling the soil was around= 2353 gram

Mass of the soil inside the core cutter = (Total mass – core cutter mass)

= (2353 – 896)

= 1457 gram

Volume of the core cutter (V) = π r^2 h

= π X 5^2 X 13

= 1021.0176 cm^3

Figure no 4.12. Weight of the core cutter after filling the soil

And density of the soil is calculated by the below formulas:

ρb = (Msoil/Volume of core cutter)

ρd = (ρb / 1 + Ꞷ)

Where,

ρb = Bulk Density

ρd = Field Density

By substituting the above values in the density formulas we get,

ρb = 1.427 gram/cm^3

ρd = 1.308 gram/cm^3

Where, the bulk density is the soil density which needs to be maintained in the chamber and field density is the actual density which is available at the site location.

From the above density the mass of the soil that can be added in the enclosed chamber can be calculated by using below formula:

$$\rho b = \frac{m}{v}$$

Where,

ρb = Bulk Density (kg/m^3)

m = Mass of the soil that can be added in the enclosed chamber (Kg)

v = Volume of the inner perforated chamber (m^3)

So from the above formula, mass of the soil that can accommodate inside the inner perforated chamber is calculated as 2998 Kg.

4.5. Setup Development:

The outer chamber fabricated for this project was made up of mild steel with the size of 1.5m*1.5m*1.5m and the material used for inner chamber was galvanized iron with 2mm of perforations and the size of that inner chamber was 1.4m*1.4m*1.25m. The front end of both outer and inner can be opened by unbolting the screws and through that portion inner chamber can be removed from the outer chamber. The below figure 4.13 shows the actual outer and inner chamber.

Figure no 4.13. Inner and outer box

The pipe material used for the above project is PVC having diameter of 100mm and with the thickness of 2 mm. The length of each pipe connected in the series was of 1.25 m long. Five pipes of length 1.25 m were connected in parallel in a single layer. And four such layers were made in order to satisfy the requirement of the load. The distance of 0.2 m was maintained between every two pipes in vertical as well as horizontal direction. So total of 27 m pipe with 38 elbows in total were utilized for the pipe structure inside the chamber. The soil which was utilized to fill the inner chamber was around 2981 Kg. The pipe arrangement before installing inside the setup is shown in the figure No 4.14. The first layer of pipe as well as soil was shown in the below figure no 4.15.

Figure no 4.14.Pipe arrangement before installation in the setup.

Figure no 4.15.First layer of soil and pipe.

The fourth/ final layer of the pipe was shown in the below figure no 4.16. And also some vertical pipes with 40 mm diameter were inserted in the soil at different locations by providing holes to it in order to maintain the moisture content in the bottom most layer. The sprinkler was used to spray the water from the top over the soil and a T-Joint was provided so that the water pipes which were connected to the water pump can directly supply the water to those smaller diameter pipes. The sprinkler arrangement after filling the entire inner chamber by soil is shown in the figure no. 4.17.

Figure no 4.16. Fourth layer of pipe with soil

Figure no 4.17. Inner chamber filled with soil including sprinkler arrangement

For the above chamber four wheels with the size of 5 inch diameter made up of PU (Polyurethene) were used. These wheels can take the load up to 3.5 tons. The PU Wheels are shown in the below figure no 4.18. From the four wheels two wheels has motion in fixed direction only while two wheels can move 360 degrees with the locking arrangement in it.

Figure no 4.18. PU Wheels for the setup

A DC blower was used for the project with 12 V power and the capacity of 1450- 3200 rpm. And a connector made up of mild steel is used to connect the blower to the inlet pipe. A dimmer was attached to the blower in order to vary the velocity of inlet air. The figure no. 4.19 shows the actual DC blower and figure no. 4.20.Shows the connector for the blower.

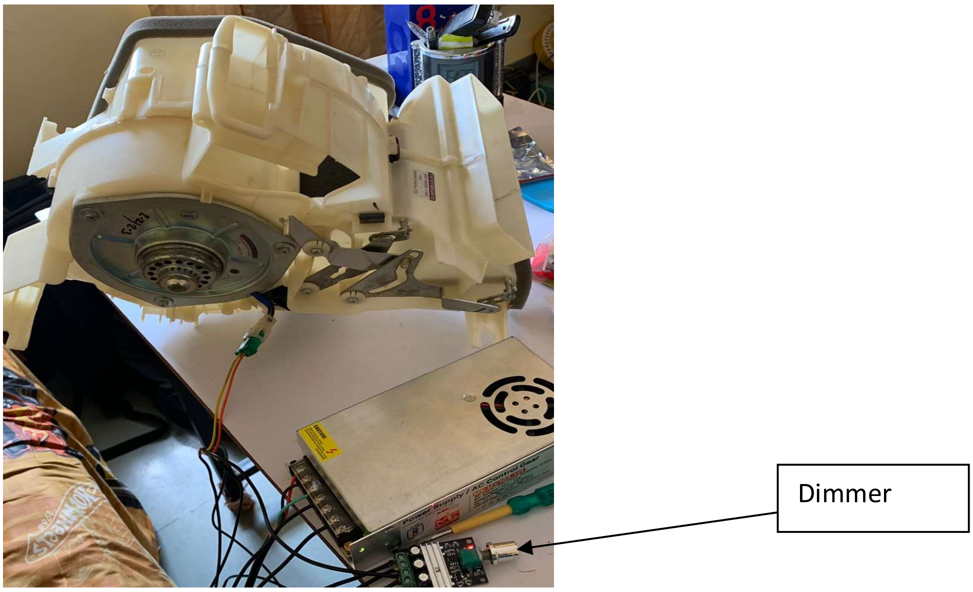

Figure no 4.19. 12 V DC Blower.

For the above setup, there are total 18 temperature sensors are used. From the 18 sensors, 12 temperature sensors were used to measure the temperature of air inside the pipe from inlet to outlet. One sensor was kept to measure the temperature of atmospheric air and rest of the temperature sensors are kept inside the soil at different level in order to measure the temperature of soil at each level along with the soil moisture sensors. There are total eight soil moisture sensors are used at different levels of the soil inside the inner chamber. For the measurement of inlet and outlet velocity MECO 961P Anemometer was used. The specifications of the above anemometer are specified below:

- MECO 961P Anemometer
- Air Velocity range- 0 to 25 m/s
- Air Velocity Accuracy : ±0.2 M/s

Probe type Temperature sensor is used for the project and the specifications of the temperature sensors are listed below:

- Model no- DS18B20
- Temperature range- -55 to 125 °C
- Accuracy- ±0.5 °C

And below are the specifications of the soil moisture sensors:

- Measuring Range- 0% to 99.9%
- Accuracy- Moisture ±3%

Figure no 4.20. Connector for Blower

The temperature sensor, soil moisture sensor and anemometer used in the project are shown in the below figure no 4.21. These temperature and soil moisture sensors are further connected to the controller connected on the 0 PCB board through multi strained wires. And the results are displayed used three displays and IOT System also used to show the readings on the firebase server. The multi strained wires from the sensors are connected to the zero PCB board as well as to the display is shown in the figure no 4.22.

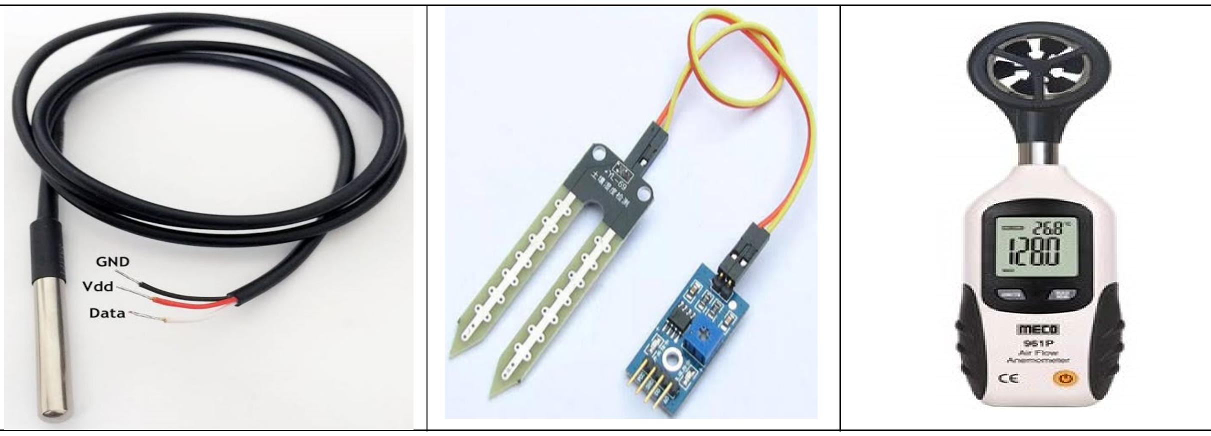

Figure no 4.21.setup accessories a) Temperature sensor b) Soil moisture sensor c) Anemometer

The Power guard is also used in the system in order to measure the power consumed by the system when connected with ETHE and without ETHE. The power guard is shown in the figure no. 4.23.

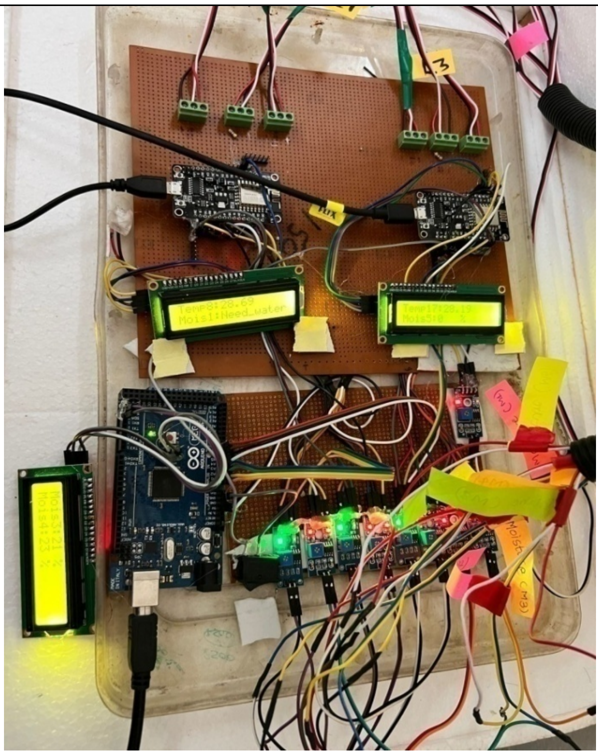

Figure no 4.22.Sensor connections with display

Figure no 4.23.Power Guard

A 250 V Water Pump is used for maintaining the moisture of the soil and the Maximum lifting height of the pump was about 1.85m. The pump is shown in the below figure no. 4.24. And the fogger was having the spraying capacity of 150 ml/ minute is shown in the figure no 4.25.

Figure no 4.24 water pump

Figure no 4.25. water sprinkler/ Fogger

For the thermal insulation of the pipe nitrile sheet of 18 mm thickness was used with thermal conductivity of 0.0034 W/m.K. The Nitrile insulation sheet is shown in the below figure no 4.26. The temperature inside the chamber is limited to some extent so thermocol is used for the outer chamber as an insulating sheet with thermal conductivity of 0.03 W/m.K. the thermocol insulation attached to the chamber is shown in the figure no 4.27.

Figure no 4.26. Nitrile sheet for pipe insulation

Figure no 4.27. Thermocol insulation for the chamber

The temperature of the soil at a certain depth from the ground remains constant throughout and it is much lesser or higher than the surface temperature. So in order to achieve this condition to the soil inside the chamber an air conditioning test rig is used. This air conditioning test rig will supply the cold or hot air as per the required environmental condition inside the chamber and will maintain the temperature of the soil. The below figure no. 4.28 shows the connection of air conditioning test rig with geothermal air conditioning test rig.

Figure no 4.28. Air conditioning test rig connections with ETHE

As the temperature of the soil is maintained at a certain value then the air blower starts. Then the air from the blower passes through the tube arrangement which is inside the chamber buried in the soil. Then the temperature of the air at the outlet of the ETHE falls if the inlet temperature is high. This reduced temperature air is further supplied to the cold storage in order to reduce the power consumption of the cold storage.

4.7. Actual Setup:

As the temperature of the soil is maintained at a certain value then the air blower starts. Then the air from the blower passes through the tube arrangement which is inside the chamber buried in the soil. As the temperature inside the soil was maintained at lower temperature and the pipe length was more so that phenomenon allows the air to transfer its heat to the soil through the pipe. The completed setup is shown in the below figure no. 4.29(a) and 4.29(b).

Figure no 4.29. (a) Complete setup arrangement view 1.

Figure no 4.29. (b) Complete setup arrangement view 2.

Chapter 5

Results and Discussion

5.1. Result Table:

From the design of experiment, analytical results of the optimum values obtained at the different cooling load conditions are shown in the below table no 5.1.

Table no 5. 1 Result Table of Optimum Values

Total Cooling Load inside the space (KW)	Optimum Length (L) (m)		Optimum Diameter (D) (m)	Optimum mass flow rate (kg/s)	Velocity of the air (m/s)	Convective heat transfer coefficient (W/m^2K)
	For cooling (m)	For Heating (m)				
0.14	7	6.9	0.1	0.01	0.26	14.07
0.23	9.4	9	0.1	0.0175	0.344	19.02
0.44	16.2	15.9	0.1	0.03	0.6	23.08
1.58	23.5	23	0.1	0.1	0.86	28.12
1.755	27.2	26	0.1	0.13	1.12	29.11
2.49	46	44.8	0.1	0.19	1.72	31.23
3.42	68	65	0.1	0.26	2.58	34.12
4.3	89	87	0.1	0.33	3.44	37.01
5.51	117	116	0.1	0.365	4.29	39.13

From the above result table, length Vs cooling load plot has also be drawn which clearly shows that with the decrease in the cooling load the length of pipe for space heating and cooling also decreases. The plot of cooling load Vs Optimum length is shown in the figure no 5.1.

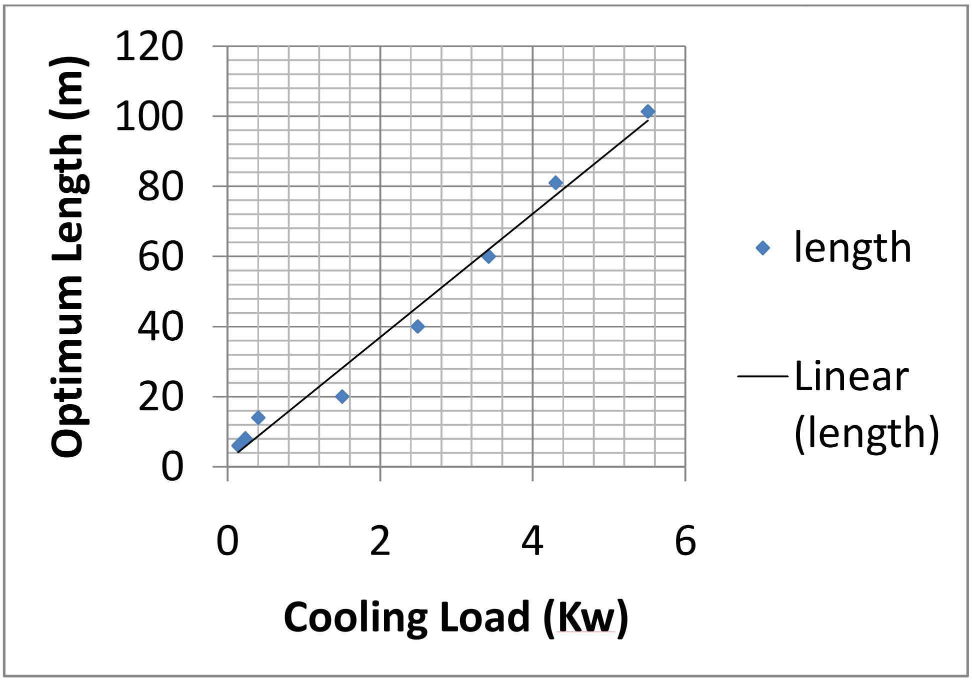

Figure no. 5. 1 Length Vs Cooling load plot

1.2. Simulation Results:

The temperature distribution contour of the pipe arrangement after applying the given boundary conditions in ANSYS FLUENT is shown in the below figure no.5.2. The minimum temperature at the outlet was obtained as 297.87 K.

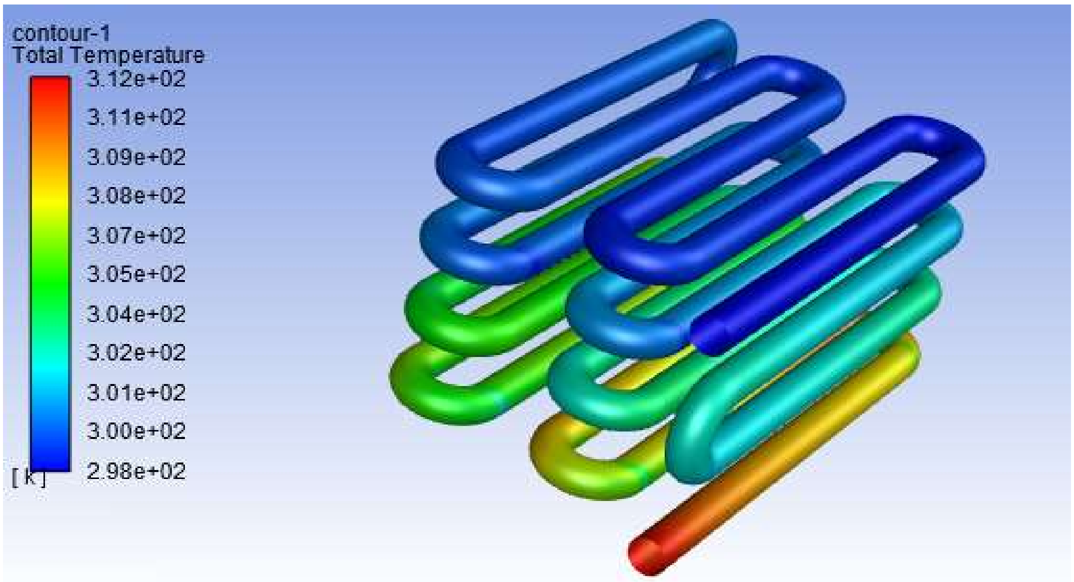

Figure no.5.2.Temperature contour

The velocity vector of the air inside the pipe is shown by the below figure no.5.3. the velocity at the outlet was reduced from 1.2 m/s to 1.1 m/s.

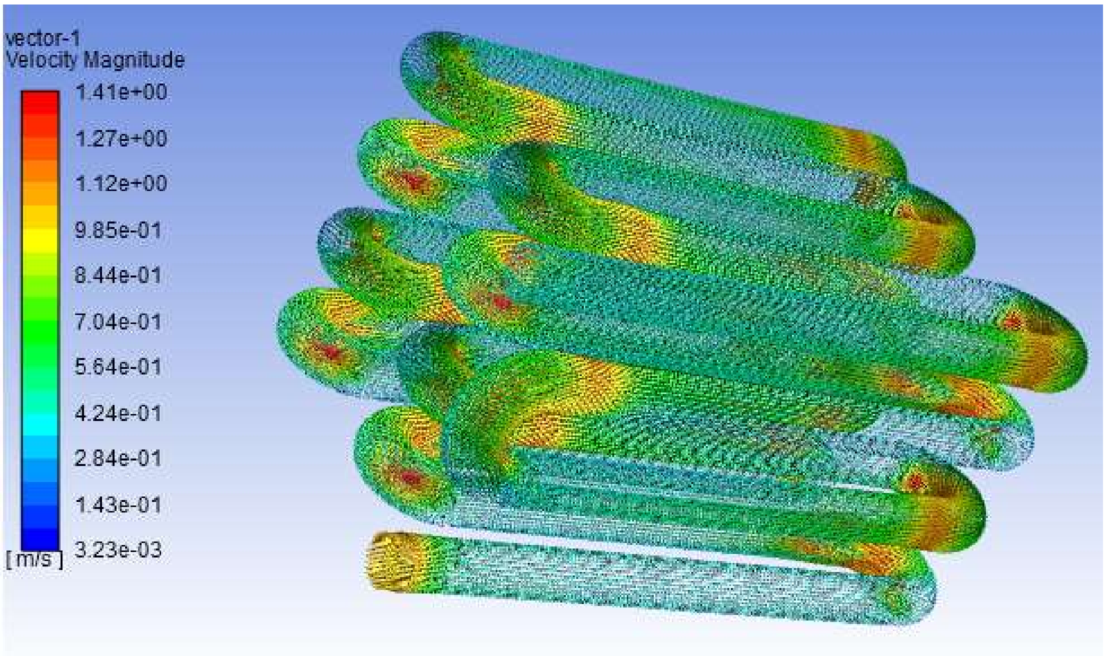

Figure no.5.3. Velocity vector

The layer wise temperature reduction of air inside the pipe is shown in the figure no.5.4.

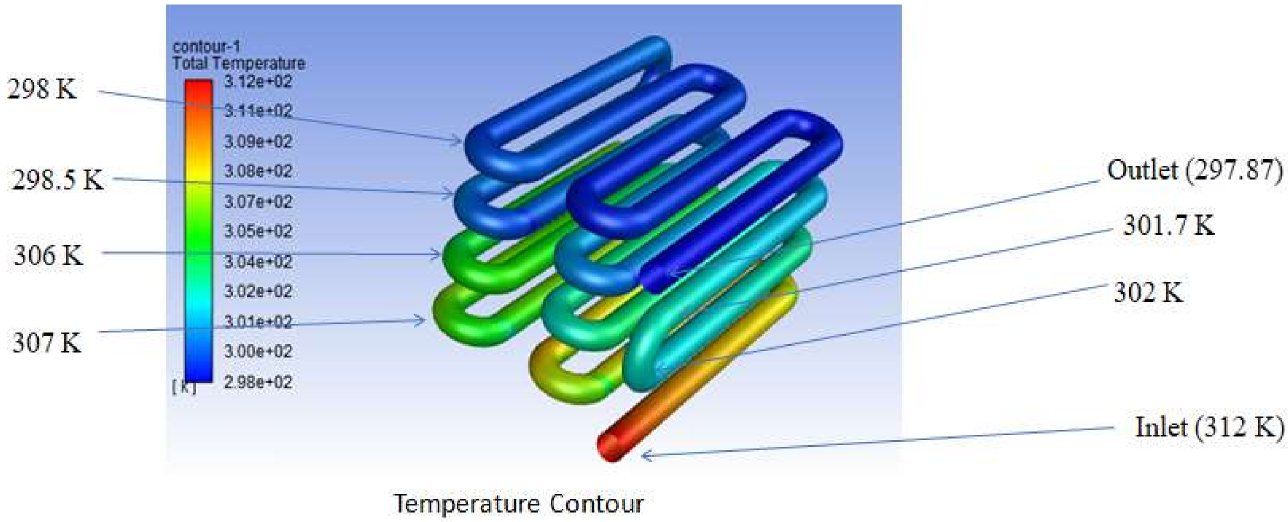

Figure no.5.4. Layer wise temperature distribution

The temperature reduction with respect to the length of pipe is shown by the figure no. 5.5.

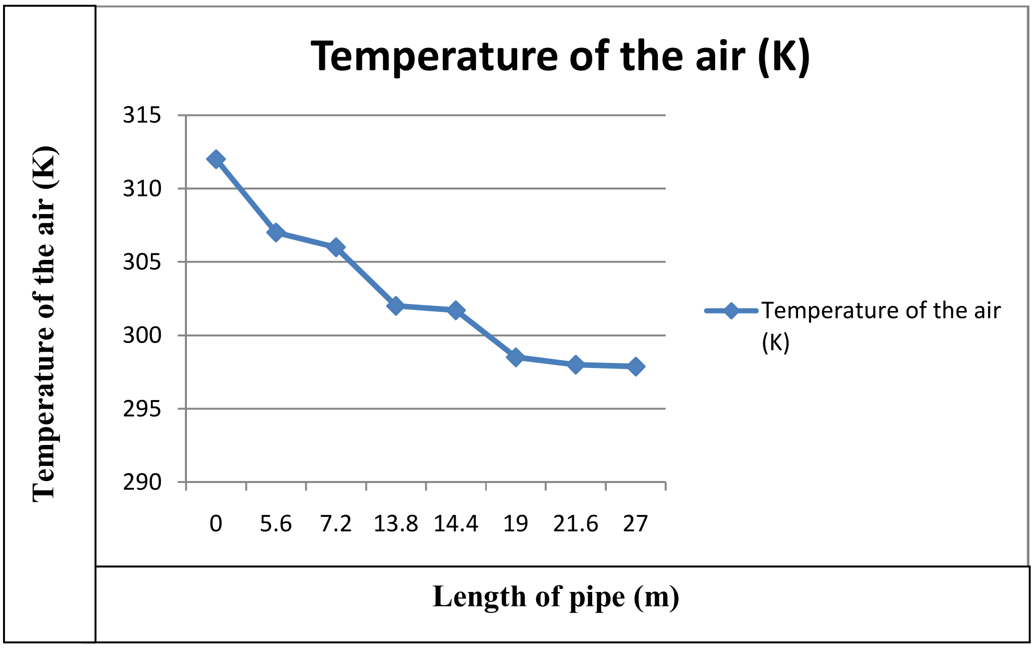

Figure no. 5. 5. Air temperature reduction along with the pipe length

The above figure no 5.5. Shows that, the temperature reduction of the air when it is passing through the heat exchange pipe.

5.3. ETHE Experimentation

The experimentation procedure should involve following aspects:

Impact on outlet air temperature,

1. By varying the moisture content in the soil
2. By varying the velocity of inlet air

The performance of ETHE can be measured by varying above aspects:

Table no 5. 2 Experimental results of ETHE test rig

Experiment no	Soil moisture content (%)	Air inlet velocities (m/s)	Soil temperature (K)	Air inlet temperature (K)	Air outlet temperature (K)	Air outlet velocity (m/s)
1.	5	0.5	298.4	308	299	0.37
		1			298.95	0.78
		1.5			299.03	1.02
		2			299.3	1.42

		2.5			299.32	1.84
		3			299.5	2.23
2.	10	0.5	298.4	308.6	298.99	0.36
		1			298.81	0.79
		1.5			299.02	1.00
		2			299.24	1.43
		2.5			299.3	1.85
		3			299.41	2.23
3.	15	0.5	298.4	310	298.85	0.38
		1			298.65	0.78
		1.5			298.72	1.03
		2			298.99	1.4
		2.5			299.09	1.83
		3			299.12	2.23
4.	20	0.5	298.4	309.6	298.83	0.38
		1			298.59	0.79
		1.5			298.62	1.01
		2			298.71	1.41
		2.5			298.94	1.83
		3			299.01	2.25
5.	25	0.5	298.4	309.3	298.7	0.37
		1			298.5	0.78
		1.5			298.53	1.02
		2			298.65	1.42
		2.5			298.79	1.84
		3			298.94	2.23
6.	30	0.5	298.4	309.2	298.97	0.36

		1			298.89	0.78
		1.5			298.92	1.02
		2			299.01	1.39
		2.5			299.04	1.80
		3			299.08	2.21

5.3.1. Steps to follow for performing above experimentation:

1) Check all the sensor readings initially, set the required soil moisture % using actuator code.
2) Maintain the temperature of soil as 298.4 K by using air conditioning test rig and required moisture level with the help of sprinkler.
3) Once the required moisture content is achieved the sprinkler will shut off automatically using the actuator.
4) Start the blower and Set the required velocity of the blower by adjusting the dimmer.
5) Sensors will show the temperature of air at each level as well as at input and output.
6) Follow the same procedure for all moisture contents as well as for all the velocities

The above results from the table are shown in the below chart of figure no 5.5 and 5.6 in a systematic way.

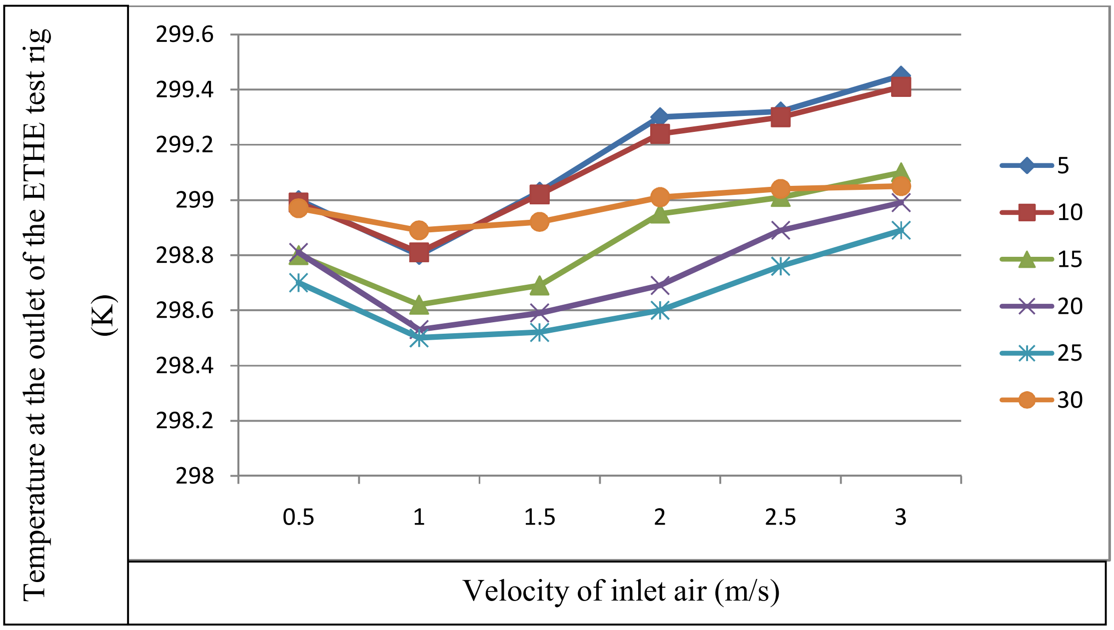

Figure no. 5. 6. Performance chart of the ETHE System

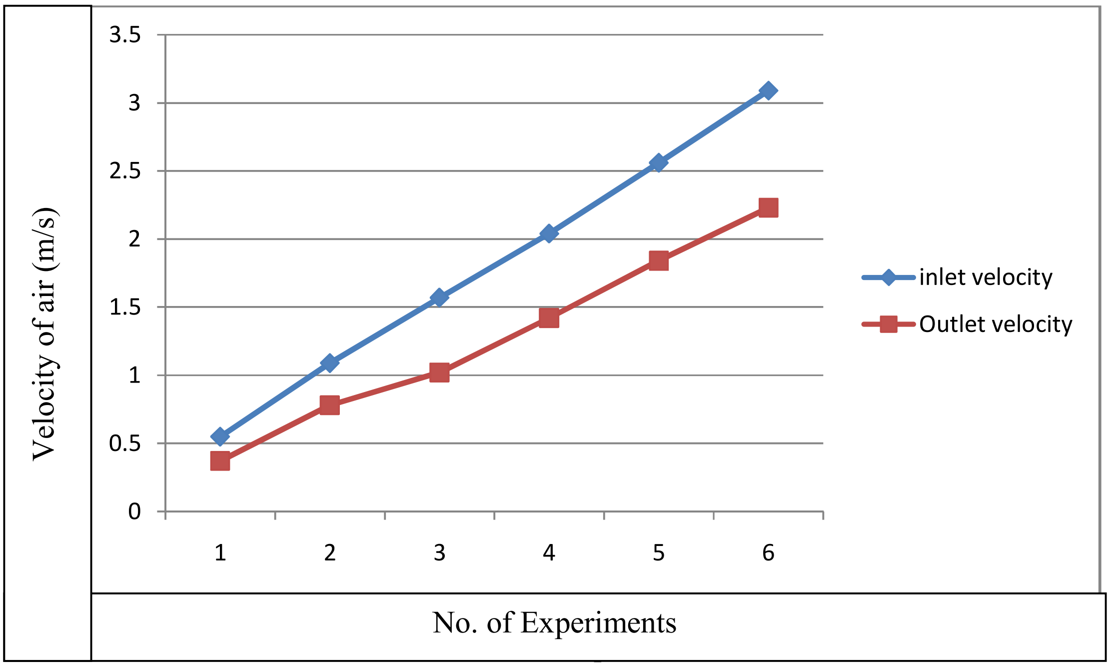

Figure no 5.7. Velocity variation at inlet and outlet

From the above experimental results and the charts, it clearly observed that soil with 25 % moisture content gives the best results. And minimum temperature was obtained when the velocity of air was maintained in between 1 m/s to 1.5 m/s.

5.4.Validation of experimental results with simulation results:

It is important to validate the simulation results with the experimental results. After maintaining the soil temperature at a constant value of 298.4 K, the obtained results from both simulation and test rig for a maximum velocity of 1.5 m/s are shown in the below table no.5.3.

Table no 5. 3 Validation of Simulation and Experimental results

Inlet air temperature (K)	Simulation Results (K)	Experimental Results (K)	Percentage Error (%)
308	298.54	298.87	1.27
308.6	298.59	298.99	1.54
310	298.84	299.47	2.3
309.6	298.76	299.42	2.49
309.3	298.70	299.36	2.5
309.2	298.67	299.21	2.06

The results shown in the above table no 5.3 are shown with the help of proper chart in the figure no 5.7. And from the results it was clearly understood that the difference between both the results are within the valid range so the results are acceptable. From the results, the percentage of error was achieved to be not more than 2.5 %.

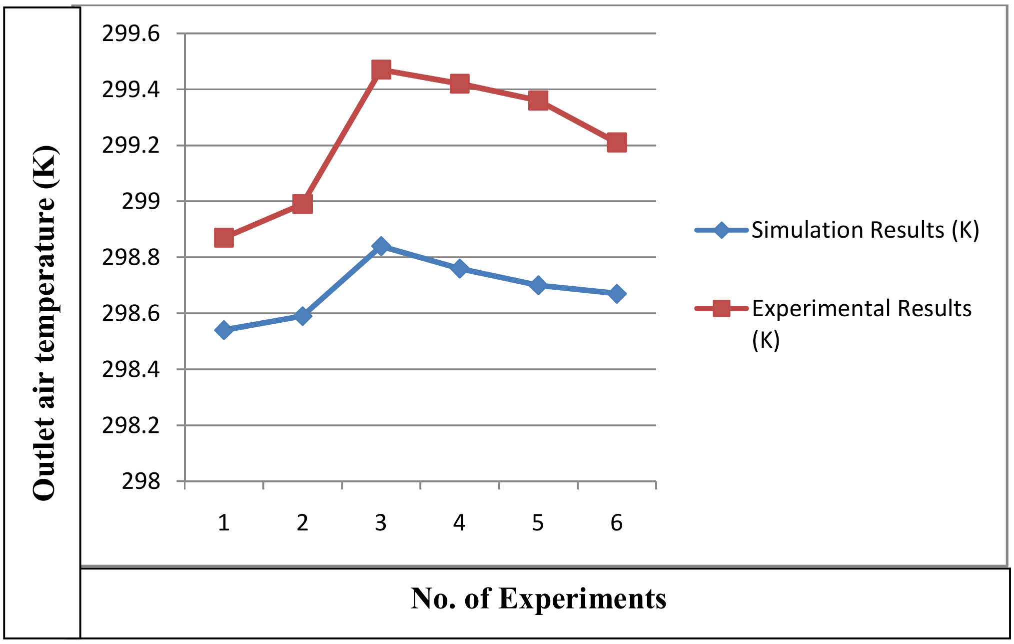

Figure no. 5. 8. Validation of Experimental results with simulation results

5.5.Temperature drop when heating medium is used at inlet:

In order to achieve the maximum temperature drop using the above geothermal air conditioning test rig, a heating element is added at the inlet of the pipe while the soil temperature was maintained at a value of 298.4K and the results showed that:

Table no 5. 4 Outlet Temperature after using heating Medium at inlet

Inlet air temperature (K)	Outlet temperature (K)		Percentage error (%)
	Simulation Results (K)	Experimental Results (K)	
313	299.01	300.03	3.7
318	299.43	301.42	6.88
323	300.39	303.03	8.43

After applying the heating medium at inlet while the velocity was kept constant for all the cases, the temperature was actually reduced by 13 Kelvin, 16 Kelvin and 19 Kelvin from the actual experimentation on the system. And the percentage of error for all the three cases was in between 3.7 % to 8.43 %.

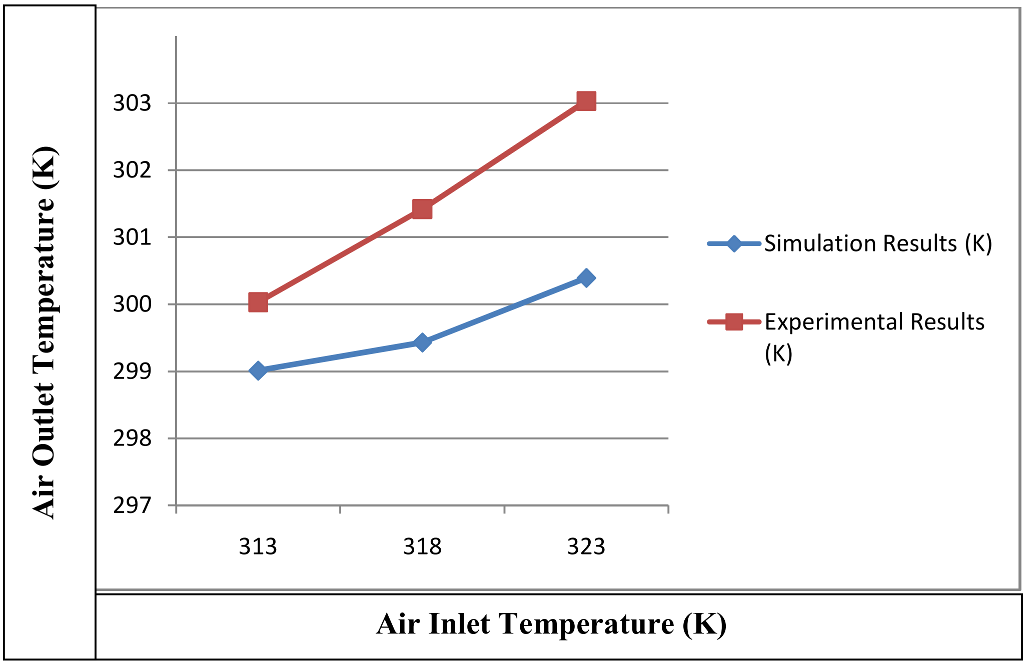

Figure no. 5. 9. Outlet temperature after adding the heating medium to the inlet

So the above graph clearly indicates that the percentage of error between experimental and simulation result is negligible and the results can be acceptable.

Chapter – 6

Cost analysis

6.1. Cost estimation of Experimental setup:

The cost of the above project is estimated as follows:

Table no 6. 1. Cost estimation of Experimental setup

Sr. No	Component	Quantity	Cost
1.	Inner and Outer Chamber Fabrication, blower reducer, air conditioning test rig connector.	1	74000
2.	Sensors and Electronic Components	1	47200
3.	PVC Piping and Plumbing Joints, Water pump and sprinkler with piping arrangement	1	11100
4.	Blower	1	5500
5.	Insulating Material – Thermocol and Nitrile sheet	33 nos	1700
6.	Anemometer	1	3000
7.	Power Guard	1	1700
8.	PU Wheels (2 fixed and 2 with brakes)	4	4720
9.	Transportation Cost		2965
		Total cost =	1,51,885/-

So from the above table, the final cost of the entire project execution and development is estimated as **Rs.1, 51,885/-**

Chapter -7

Conclusion and Future Scope

7.1. Conclusion:

- The above study uses Taguchi Optimization method in order to achieve maximum information from minimum number of experiments and also the best level of each parameter.
- The ANNOVA Concept (Analysis of Variance) was used in order to achieve the maximum impact of each parameter on the size of the air conditioning pipe. The length of the pipe was calculated for different volumes and loads for both heating and cooling.
- From the analytical results, it was observed that for a load of 1.755 KW the length of pipe for space cooling was about 27 m and convective heat transfer coefficient is 29.11 W/m2K.
- The design of pipe as well as outer and inner chamber was designed using AUTODESK FUSION 360 software. And CFD analysis was carried out over the pipe geometry using ANSYS FLUENT software.
- From the CFD analysis results, Temperature drop of around 14 K was achieved when the soil temperature was maintained at 297 K.
- Pipe arrangement was arranged inside the chamber of 1.5m*1.5 m*1.5 m. the outer chamber is fully insulated and made of mild steel whereas the inner chamber is made of Perforated sheets made up of Galvanized Iron.
- Air conditioning test rig was used to maintain the temperature soil.
- The experimentation on the geothermal air conditioning test rig was carried by varying the inlet air velocity, soil moisture content and adding heating source at the inlet and the results are further validated.
- From the results it was concluded that, soil with 25 % moisture content and air with 1 to 1.5 m/s velocity gives the best results.

7.2. Future scope:

1. Experimentations should be carried out by changing the backfilling material and achieve better composition of the backfilling materials.
2. The blower which is used to provide input air to the ETHE test Rig can be powered using Solar Energy in order to reduce dependency on conventional energy sources and focus more on using the sustainable resource of energy.
3. The above system should be used for high capacity HVAC applications like cold storages, central air conditioners in order to achieve power saving.

References:

1. Farheen Bano Examining the Role of Building Envelope for Energy Efficiency in Office Buildings in India 10.5923/j.arch.20160605.01 Architecture Research 2016, 6(5): 107-115.
2. Agrawal, K. K., Misra, R., Agrawal, G. D., Bhardwaj, M., & Jamuwa, D. K. (2019). Effect of different design aspects of pipe for earth air tunnel heat exchanger system: A state of art. International Journal of Green Energy, 16(8), 598-614.
3. Agrawal, K. K., Misra, R., & Agrawal, G. D. (2021). CFD simulation study to evaluate the economic feasibility of backfilling materials for ground-air heat exchanger system. Geothermics, 90, 102002.
4. Misra, R., Bansal, V., Agrawal, G. D., Mathur, J., & Aseri, T. (2013). Transient analysis based determination of derating factor for Earth Air Tunnel Heat Exchanger in winter. Energy and Buildings, 58, 76-85.
5. Singh, B., Asati, A. K., & Kumar, R. (2021). Evaluation of the cooling potential of earth air heat exchanger using concrete pipes. International Journal of Thermophysics , 42(2), 1-19.
6. Pandey, N., Murugesan, K., & Thomas, H. R. (2017). Optimization of ground heat exchangers for space heating and cooling applications using Taguchi method and utility concept. Applied Energy, 190, 421-438.
7. D'Agostino, D., Marino, C., & Minichiello, F. (2019). Earth to-air versus air-to-air heat exchangers: A numerical study on the energetic, economic, and environmental performances for Italian office buildings. Heat Transfer Engineering.
8. Benrachi, N., Ouzzane, M., Smaili, A., Lamarche, L., Badache, M., & Maref, W. (2020). Numerical parametric study of a new earth-air heat exchanger configuration designed for hot and arid climates. International Journal of Green Energy, 17(2), 115-126.
9. Abbaspour-Fard, M. H., Gholami, A., & Khojastehpour, M. (2011). Evaluation of an earth-to-air heat exchanger for the north-east of Iran with semi-arid climate. International Journal of Green Energy, 8(4), 499-510.
10. Lin, J., Nowamooz, H., Braymand, S., Wolff, P., & Fond, C. (2020). Impact of soil moisture on the long-term energy performance of an earth-air heat exchanger system. Renewable Energy, 147, 2676-2687.

11. Amanowicz, Ł., & Wojtkowiak, J. (2021). Comparison of single-and multipipe earth-to-air heat exchangers in terms of energy gains and electricity consumption: A case study for the temperate climate of central europe. Energies, 14(24), 8217.
12. W. Morshed, L. Abbas, H. Nazha, Heating performance of the PVC earthair tubular heat exchanger applied to a greenhouse in the coastal area of west Syria: An experimental study, Thermal Science and Engineering Progress (2021). doi:https://doi.org/10.1016/j.tsep.2021.101000
13. N. Sakhri, Y. Menni, H. Ameur, "Impact of the environmental conditions on the efficiency of earth to air heat exchangers under various configurations" International Journal of Environmental Science and Technology https://doi.org/10.1007/s13762-021-03165-w
14. KK Agarwal et.al "CFD simulation study to evaluate the economic feasibility of backfilling materials for ground air heat exchanger system" doi:https://doi.org/10.1016/j.geothermics.2020.102002.
15. D. Namgial et.al "Performance of Thermo Hydraulic Designed Single Pass Earth Air Heat Exchanger" : IJAEB: 12(1): 55-62, March 2019 DOI: 10.30954/0974-1712.03.2019.9
16. A.k.Patel et.al "CFD Analysis of Geothermal Heat Exchanger at Different Orientation" doi= 10.24113/ijoscience.v5i7.177
17. Trilok Singh Bisoniya "Design of earth–air heat exchanger system" Bisoniya Geothermal Energy (2015) 3:18 DOI 10.1186/s40517-015-0036-2
18. Nikhil Jagtap et.al. "Design and Transient Analysis of Earth-Air Heat Exchanger" 284| AMET_0068 @ MIT College of Engineering, Pune, Vol.04, Special Issue AMET-2018. DOI : 10.18231/2454-9150.2018.1453
19. M.d. Paepe et.al "thermo- hydraulic design of earth tube heat exchanger" Energy and buildings 35 (2003) 389-397.
20. https://theconstructor.org/geotechnical/dry-density-of-soil-by-core-cutter-method/2680